

ORIGINAL RESEARCH

3 OPEN ACCESS



A laminin α4–CD8⁺ T cell axis shapes the prognostic impact of macrophages and regulatory T cells in early-stage colorectal cancer

Elena Nonnast^a, María Jesús Fernández-Aceñero^b, Tirso Pons^a, María Pilar Díaz Suárez^b, Carlos Óscar S. Sorzano^c, Emilia Mira^a, and Santos Mañes pa

^aDepartment of Immunology and Oncology, Centro Nacional Biotecnología (CNB-CSIC), Madrid, Spain; ^bDepartment of Surgical Pathology, Hospital Universitario Clínico San Carlos, Madrid, Spain; ^cBiocomputing Unit and Computational Genomics, Centro Nacional Biotecnología (CNB-CSIC), Madrid, Spain

ABSTRACT

The crossing of the endothelial basement membranes (BMs) is a limiting step for leukocyte diapedesis. Heterotrimeric laminins (LMs) containing α 4- and α 5-chains are major BM components with opposite effects on transendothelial migration. Here, we examined whether LMa4 levels influence intratumor accumulation of specific immune cells and their impact on prognosis of early-stage colorectal cancer (CRC). Using two independent patient cohorts, we found that LMα4 expression positively correlated with intratumor infiltration of CD8⁺ T cells and macrophages, but not with regulatory T (Treg) cells. Kaplan-Meier and multivariate Cox regression analyses identified CD8⁺ T cell density as the strongest independent prognostic factor associated with reduced tumor relapse in both cohorts. While intratumor macrophage and Treg cell densities alone were not independently associated with prognosis, their abundance modulated outcomes specifically in tumors with high CD8⁺ T cell infiltration, with macrophage-rich tumors showing improved outcomes and Treg cell-enriched tumors exhibiting worse prognosis. Analysis of The Cancer Genome Atlas (TCGA) COAD cohort confirmed the positive correlation of LM α 4 expression with both CD8 $^+$ T cell and macrophage infiltration, an association that was independent of the CRC clinical stage. Our findings suggest a subtype-specific effect for LMa4 in intratumor leukocyte infiltration, and underscore the prognostic interactions among CD8⁺ T cells, Treg cells and macrophages in earlystage colorectal cancer.

ARTICLE HISTORY

Received 30 October 2024 Revised 5 August 2025 Accepted 6 August 2025

KEYWORDS

leukocyte; T cell; myeloid cell; transmigration; diapedesis; immunosurveillance; immunotherapy; prognosis; extracellular matrix; Basement membrane; colorectal carcinoma

Introduction

Colorectal cancer (CRC) is a major health concern globally, with rising incidence among younger adults and prognosis largely tied to the stage at diagnosis. Despite advances in molecular classification of CRC, ^{1–3} prognosis still relies primarily on histological analysis of tumor penetration, as defined by the American Joint Committee on Cancer (AJCC) and the Union for International Cancer Control (UICC) TNM staging system, along with tumor differentiation. ⁴ Although this framework provides valuable insights, there is a clinical need to improve prognostic accuracy, especially in early-stage CRC. The risk/benefit balance of chemotherapy must be carefully balanced, restricting its use to high-risk cases, such as pT4aN0 tumors or those with perforation at diagnosis.

Growing evidence underscores the tumor microenvironment (TME), particularly intratumor immune cells, as a key determinant of CRC outcomes. Immune cells -including regulatory T cells (Tregs), macrophages, myeloid-derived suppressor cells (MDSCs), and CD8⁺ cytotoxic lymphocytes- are not passive bystanders but active players in disease progression and therapy response. Several studies suggest that quantifying specific immune populations may serve as a prognostic marker of CRC.^{5–7} Combining AJCC/UICC staging with total CD3⁺ and effector CD8⁺ T cell density improves prognostic accuracy in both early-and advanced-stage CRC patients.^{8,9} However, the immune score's clinical utility remains debated, as technical challenges hinder its application to the clinical routine.

CONTACT Santos Mañes smanes@cnb.csic.es Department of Immunology and Oncology, Centro Nacional de Biotecnología, Darwin 3, Madrid 28049, Spain

B Supplemental data for this article can be accessed online at https://doi.org/10.1080/2162402X.2025.2546181

This limited clinical impact may stem from gaps in our understanding on the prognostic value of specific immune subsets and their interactions within the TME. A key example is the dual role of Treg cells in CRC prognosis. High intratumor Treg cell density has been linked to improved relapse-free survival (RFS) and overall survival (OS), tell an in silico analysis of public datasets identified a Treg-associated gene signature predicting poor OS. The molecular basis for this paradox remains unclear. Treg cells may improve prognosis by dampening inflammation that fuels CRC progression, but could also worsen outcomes by hampering local or systemic anti-tumor T cell responses. This dualism might reflect distinct Treg subpopulations or interactions with the gut microbiota.

The prognostic value of tumor-associated macrophages (TAM) in CRC remains controversial. TAMs exhibit a notable phenotypic and functional diversity, with distinct subsets influencing tumor progression differentially. Experimental models suggest that M1-like TAMs have a pro-inflammatory, tumor-suppressive phenotype, whereas M2-like TAMs promote a tolerogenic TME, angiogenesis, and tumor progression. A meta-analysis of 27 studies involving over 6,000 patients found that increased CD68⁺ TAM density correlated with favorable prognosis, though no differences were observed when stratified by M1 and M2 subset. Pemarkably, TAM diversity is highly influenced by environmental factors, suggesting that their function may depend on interactions with other immune cells in the TME.

Another important determinant of intra-tumor immune cell accumulation is the molecular cues governing leukocyte diapedesis. To infiltrate tumors, immune cells must traverse vascular or lymphatic endothelial barriers *via* transendothelial migration. This process requires coordinated interactions between diapedesis-associated receptors, integrins, and chemokines expressed by both leukocytes and endothelial cells.²¹ These interactions enable leukocytes to adhere and undergo morphological changes required for migration. Nonetheless, after crossing the endothelium, leukocytes encounter a second barrier, the endothelial basement membrane (BM), an extracellular matrix structure composed of type IV collagen and the laminin (LM) networks.²²

Laminins are heterotrimeric proteins composed of α (α 1- α 5), β (β 1- β 3), and γ (γ 1- γ 3) subunits. Although 60 trimeric combinations are possible, only 16 LM isoforms have been biochemically confirmed. The α -chains contain most of the determinants for cell interaction by binding integrins and glycosaminoglycans. Therefore, distinct LM α -chains impinge attached cells with particular functional and biomechanical properties due to the induction of specific signal transduction pathways. In endothelial BMs, the predominant α -isoforms are LM α 4 (LAMA4 gene), found in all blood vessels, and LM α 5 (LAMA5 gene), expressed in capillaries and venules. These isoforms primarily combine with β 1- and γ 1-chains to form LM-411 (α 4 β 1 γ 1) and LM-511 (α 5 β 1 γ 1), respectively. While LM-411 shows homogeneous distribution in the BM, LM-511 forms patchy regions. This spatial pattern may be relevant in leukocyte diapedesis, since immune cells preferentially transmigrate through areas with low LM-511 levels. The LM-411/LM-511 balance is critical for immune regulation in both homeostasis and cancer. High LM-411/LM-511 ratios in the BM of high endothelial venules promote Treg cell infiltration into lymph nodes, suppressing alloreactivity. In cancer models, LM-411 upregulation in tumor vasculature is linked to enhanced antitumor responses and reduced tumor progression, whereas LM-511 associates with a pro-tumorigenic inflammatory TME.

Here, we studied whether LM $\alpha 4$ -chain expression correlates with CD8⁺, Treg and CD68⁺ cell infiltration and its impact on early-stage CRC prognosis. LM $\alpha 4$ -chain levels positively correlated with intratumor CD8⁺ T cells and CD68⁺ macrophages but not with Treg cells, a pattern also observed in the TCGA COAD cohort across all clinical stages. In two independent CRC cohorts, multivariate Cox regression identified intratumor CD8⁺ T cell abundance as the strongest independent factor linked to reduced relapse risk. Macrophages and Tregs influenced prognosis only in tumors with high CD8⁺ T cell density, suggesting functional interactions within the TME. These results reveal a cell type-specific effect of LM $\alpha 4$ on diapedesis and highlight the potential relevance of CD8⁺, Treg and macrophage interactions in early-stage CRC prognosis.

Materials and methods

Human samples

The study cohort comprised 95 patients diagnosed with early-stage colorectal cancer (CRC) between 2000 and 2010, selected from the surgical pathology database of the Hospital Fundación

Jiménez Díaz (Madrid, Spain). The validation cohort consisted of 226 patients with stage II CRC adenocarcinomas diagnosed between 2008 and 2018 at Hospital Infanta Leonor (Madrid, Spain). Tissue microarrays (TMA) were assembled using two 1 mm cores from representative tumor areas selected from formalin-fixed paraffin-embedded blocks. Two pathologists independently reviewed the hematoxylin and eosin - stained sections from each resection specimen to select the most representative regions and assess key histopathological features. Adhering to ASCO and ESMO guidelines, none of the patients received neoadjuvant or adjuvant chemotherapy prior to disease recurrence.³¹ Recurrence rates and time to relapse were consistent with other studies for this tumor stage. 32,33 Demographic and clinicopathological characteristics, including sex, patient age at diagnosis, tumor location, pT stage and tumor grade for both cohorts, are summarized in Supplementary Table S1 and Table S2.

Gene expression data and clinical information from the COAD cohort from The Cancer Genome Atlas (TCGA) were downloaded from the NCI's Genomic Data Commons (GDC) using the UCSC Xena Browser tool (https://xena.ucsc.edu/).34 This included log2(count +1) and log2(TPM +1) expression data, sample phenotypes, and survival status. Log2-transformation was reversed for TPM (transcript per million mapped reads) data using Morpheus software (https://software.broadinstitute.org/mor pheus). A total of 41 normal and 472 colon cancer samples were analyzed. To estimate immune cell infiltration, the cohort was stratified by tumor stage based on TCGA clinical information. For statistical power, tumors were grouped as localized (stage I-II), and advanced (stage III-IV). Demographic and clinicopathological data for both cohorts are in Suppl. Table S3 and S4, respectively. To ensure consistency, tumors in the hepatic flexure were classified as right colon, and those in the splenic flexure as left colon. Cases with incomplete annotations were excluded.

Quantification of intratumor immune cells

Archival formalin-fixed paraffin-embedded blocks diagnosed with CRC were retrieved from the Department of Surgical Pathology of both hospitals and marked to select representative areas from the tumor. The TMA was serial sectioned, slides deparaffinized and treated with pre-warmed (95° C) citrate buffer (pH 6.0, 20 min) and then incubated with anti-LAMA4 (clone HPA015693, Sigma-Aldrich), anti-CD8 (clone C8/144B, Dako), anti-FOXP3 (clone EPR22102-37, Abcam) or anti-CD68 (KP1, Agilent) antibodies, followed by appropriate peroxidase-labeled secondary antibodies. The reaction was developed with diaminobenzidine, and counterstained with hematoxylin. Appropriate tissues were used as positive and negative controls. Staining was evaluated using a Leica DM500 microscope by a single pathologist blinded to experimental data. For LAMA4, a z-score was calculated (range 0-300) as the product of the intensity of the staining (1-3) and the percentage of stained cells. The number of FOXP3+, CD8+, and CD68⁺ cells was determined in 1 mm².

For the COAD cohort, immune cell abundance was determined from whole RNAseq data using TIMER2.0 (http://timer.comp-genomics.org/) algorithm. 35

Simultaneous detection of intratumor immune cells by immunofluorescence

Immunofluorescence (IF) staining was performed on deparaffinized CRC tissue sections following heat-induced antigen retrieval in Tris 10 mM, EDTA 1 mM buffer (pH 9.0) for 20 minutes. Sections were incubated with a combination of three primary antibodies: mouse anti-hCD8, rabbit antihFoxP3, and rat anti-hCD68 (clone 186F9B4, HistoSure). Detection of CD68 and FoxP3 was achieved using fluorescently conjugated secondary antibodies Alexa Fluor 488-conjugated goat antirat IgG and Alexa Fluor 647-conjugated goat anti-rabbit IgG (Thermo Fisher Scientific), respectively. For CD8 detection, signal amplification was performed using biotinylated goat anti-mouse IgG (Jackson ImmunoResearch) followed by streptavidin - Cy3 (Jackson ImmunoResearch). Nuclei were counterstained with DAPI, and sections were mounted using ProLong Gold Antifade Mountant (Invitrogen). Images were acquired with a Leica TCS SP8 STED 3X multispectral confocal microscope with an HC PL APO CS2 63×/1.40 NA oil immersion objective and processed using FIJI (ImageJ) software.

Statistical analysis

Qualitative data are presented as percentages and absolute numbers, quantitative data as mean ± SEM, unless otherwise indicated; the number of replicates is given in figure legends. For the study and validation cohorts, cases were divided into low and high groups for LMα4, FOXP3⁺, CD8⁺, and CD68⁺ cells using a receiver operating characteristic (ROC) curve approach³⁶; cutoff scores for each marker are indicated in the text. In the case of the COAD cohorts, ROC curves could not be established to discriminate tumors with high or low levels of immune cells. Correlation analyses between the different variables were performed using the non-parametric Spearman's rank correlation coefficient (GraphPad Prism v.10; GraphPad Software, LLC). The outcome measure used for the study cohort was RFS, defined as the time elapsed between surgical resection of the tumor with a curative intent and recurrence of disease in months. For the COAD cohorts, the outcome measure was OS. Kaplan-Meier curves were compared with log-rank tests; hazard ratios (HR) and 95% confidence intervals (CI) were also determined using GraphPad Prism. We used a multivariate Cox proportional hazards model to assess the relationship between tumor recurrence (study and validation cohorts) or OS (COAD cohort) and time to recurrence or time to death. The analysis was conducted using the 'CoxPHFitter' function from the lifelines Python package v0.30.0 (https://doi.org/ 10.5281/zenodo.1252342) with default parameters, which estimate the baseline hazard non-parametrically via Breslow's method and handle ties using Efron's method. In all cases, differences were considered statistically significant when the p-value was < 0.05.

Results

Laminin α4 levels correlate with intratumor CD8⁺ T cells and macrophages, but not tregs

The number of CD8⁺ T cells, Treg cells (FoxP3⁺) and macrophages (CD68⁺) was determined by direct counting of positively stained cells in TMA from the study cohort. LM α 4-chain expression was detected on the same TMA, and normalized as z-scores. The median LM α 4 z-score was 95.1 (range 10–300), and ROC analysis defined a cutoff of 70 to balance sensitivity and specificity. Among immune cell subsets, CD8⁺ T cells were the predominant infiltrating population, whereas Tregs were the least abundant (Figure 1(A)).

A significant positive correlation was found between LM α 4-chain z-score and intratumor CD8⁺ T cell density (r = 0.26, p < 0.01; Figure 1(B)), with higher LM α 4 z-scores linked to increased CD8⁺ T cell infiltration (Figure 1(C)). This association was not observed for CD8⁺ lymphocytes in the lamina propria (r = -0.07, p = 0.46; Supplementary Figure S1), suggesting a tumor-restricted effect. In contrast, LM α 4 expression did not correlate with intratumor Treg cell density (r = 0.04, p = 0.64; Figure 1(D)), and Treg cells were evenly distributed between tumors with high and low LM α 4-chain expression tumors (Figure 1 (E)). Moreover, no correlation was found between intratumor Treg and CD8⁺ T cell densities (r = 0.01, p = 0.86; Figure 1(F)), suggesting distinct recruitment or retention mechanisms for these subsets.

We next investigated the relationship between LM α 4-chain levels and myeloid cell infiltration. LM α 4 z-score correlated with intratumor macrophage density (r = 0.24, p = 0.02; Figure 1(G)). Macrophage infiltration also correlated with intratumor CD8⁺ T cell density (r = 0.29, p = 0.003; Figure 1(H)), but not with Treg cell abundance (r = 0.19, p = 0.07; Figure 1(I)). These findings point to a selective association between LM α 4-chain expression and tumor infiltration by CD8⁺ T cells and macrophages, but not Treg cells.

We further conducted immunofluorescence analyses to assess the spatial distribution of CD8⁺ T cell, Tregs and macrophages within the tumor microenvironment. A key limitation of these analyses was the low abundance of FoxP3⁺ Treg cells in the majority of tumors examined. Regardless of the relative abundance of each immune cell subtype, this analysis did not reveal any consistent spatial organization or notable colocalization among the three populations. (Supplementary Figure S2).

Prognostic value of intratumor CD8, treg cells and macrophages in the study cohort

CD8⁺ T cells have been previously implicated in favorable outcomes in stage II CRC. In our study cohort, Kaplan-Meier analysis based on CD8⁺ T cell density showed that higher levels were associated with increased relapse-free survival (RFS; p = 0.004, Log-rank test for trend; Supplementary Figure S3). ROC

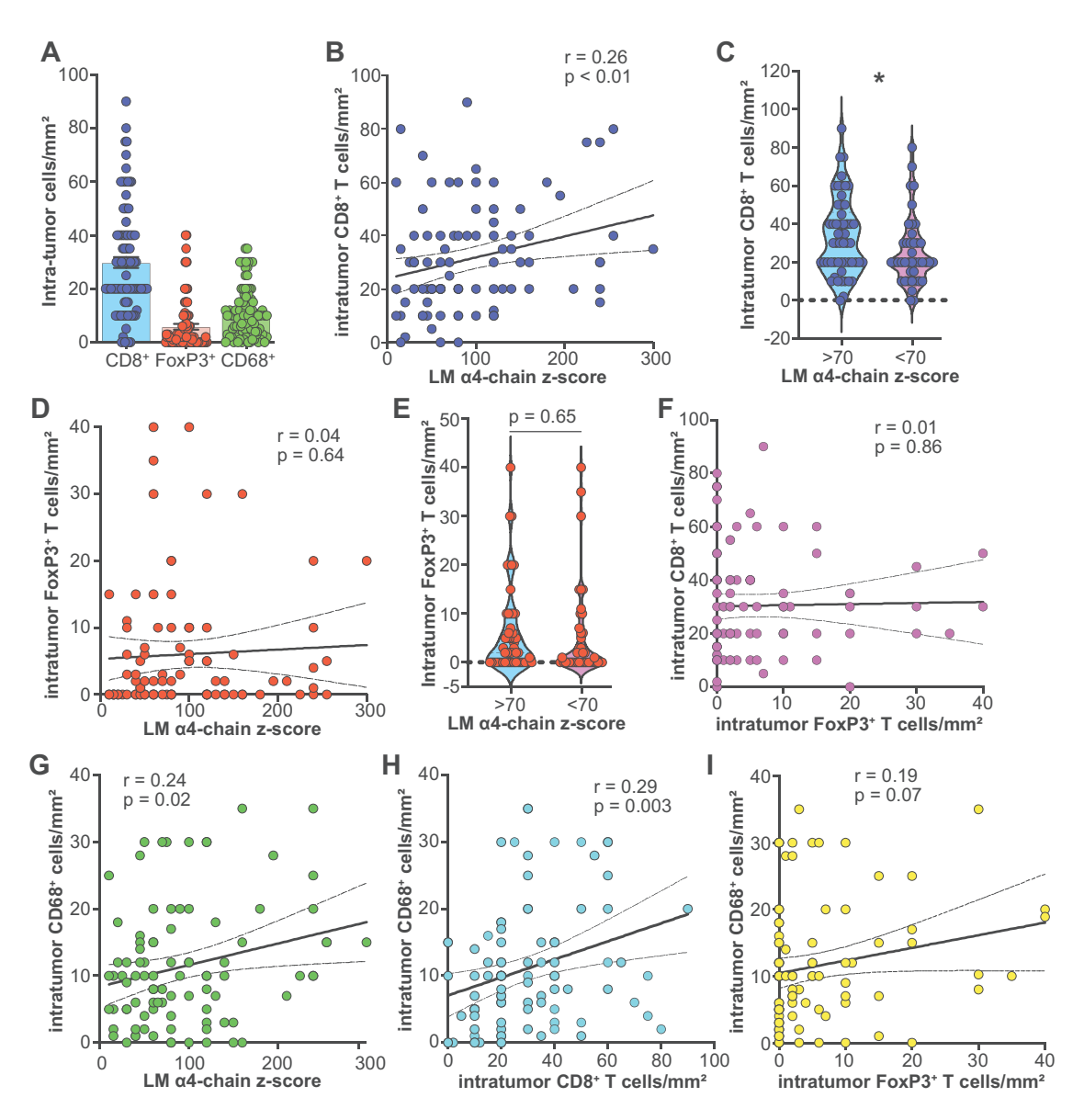


Figure 1. LM α4-chain levels positively correlate with intratumor CD8⁺ T cell and macrophages but not with Treg cells. A) number of immune cells per mm² determined by counting in each TMA of the study cohort. B) correlation between the LM α4-chain z-score and intraepithelial CD8⁺ T cells in each tumor. C) violin plots with individual data points illustrating the number and distribution of intratumor CD8⁺ T cells/mm² in tumors classified as LM α4-chain-high (z-score > 70) or -low (z-score < 70). D) correlation between the LM α4-chain z-score and intraepithelial Treg cell numbers. E) violin plots showing the distribution of Treg cells in LM α4-chain-high and -low tumors. F) correlation between intratumor Treg and CD8⁺ T cell density. G-I) correlations between intratumor macrophages and LM α4-chain z-score (G), CD8⁺ T cells (H) and Treg cells (I). Dotted lines represent 95% confidence intervals. p-values are indicated in the figures. Statistical tests: two-tailed Pearson's correlation coefficient (B, D, F-I), and two-tailed Student's *t*-test (C, E); *p < 0.05.

curve analyses identified optimal prognostic thresholds: \geq 30 cells/mm² for CD8+ T cells, and > 10 cells/mm² for Treg cells and macrophages. Using these cutoffs, Kaplan-Meier analysis indicated that high intratumor CD8+ T cell density was significantly associated with reduced relapse risk (HR = 0.40, 95% CI = 0.19–0.82, p = 0.01; Figure 2(A)), as was high macrophage density (HR = 0.41, 95% CI = 0.19–0.87, p = 0.016; Figure 2(B)). In contrast, Treg cell density showed did not significantly impact RFS (HR = 1.25, 95% CI = 0.53–2.93, p = 0.62; Figure 2(C)). These findings are consistent with previous observations linking elevated LM α 4 expression -which associates with CD8+ T cell and macrophage infiltration- with favorable prognosis in CRC.²⁹

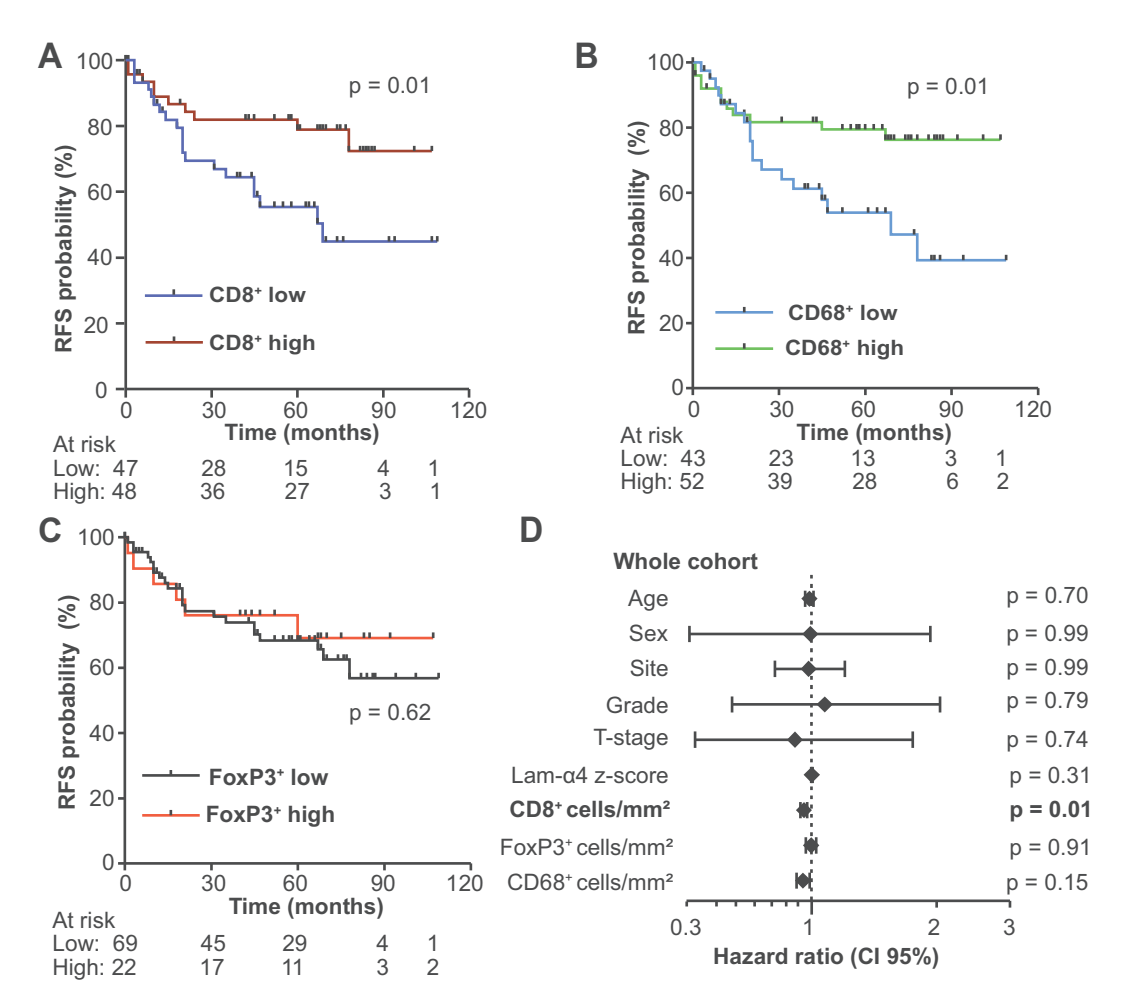


Figure 2. The density of CD8⁺ T cells and macrophages, but not Treg cells, is linked to patient prognosis. (A–C) Kaplan-Meier RFS curves and number of patients at risk in the study cohort, based on groups defined by high or low intratumor abundance of CD8⁺ T cells (A), CD68⁺ macrophages (B), or Treg (FoxP3⁺) cells (C). p-values were determined using the log-rank test. (D) multivariate Cox regression analysis of clinical and immune parameters in the CRC study cohort. The hazard ratio and 95% confidence interval (Cl) are shown. Additional data from the correlation analysis are provided in Suppl. Table S5.

To assess independent prognostic contributions, we performed multivariate Cox proportional hazards modeling, which identified intratumor CD8⁺ T cell density as the sole independent predictor of improved RFS (HR = 0.96, 95% CI: 0.93–0.99, p = 0.01; Figure 2(D) and Supplementary Table S5). The high concordance index (0.73) further supports the predictive performance of CD8 T cell infiltration in early-stage CRC.

Interactions between CD8⁺ T cells, macrophages and Treg cells in CRC prognosis

Since high CD8⁺ T cell infiltration emerged as an independent favorable prognostic factor, we next examined whether its prognostic effect was modulated by the presence of Treg cells or macrophages, which are known to influence CD8⁺ T cell activity. Tumors were stratified by CD8⁺ T cell density, and RFS was analyzed in relation to Treg and macrophage infiltration. Stratification was necessary to address potential violations of the proportional hazards assumption, as the strong impact of CD8⁺ T cell infiltration on RFS might cause risk to vary over time. This approach allows the development of independent RFS models within high and low CD8⁺ T cell contexts, while maintaining analytical validity.

Although Treg cell density alone lacked prognostic significance, Kaplan-Meier analysis revealed a trend toward worse outcomes in tumors with high CD8⁺ T cell infiltration when Treg cell density was elevated

(HR = 2.69, 95% CI = 0.56–12.82, p = 0.13; Figure 3(A)), but not in tumors with low CD8⁺ T cell infiltration (HR = 0.46, 95% CI = 0.17–1.21, p = 0.19; Figure 3(B)). Conversely, high macrophage infiltration was associated with a trend toward improved prognosis in high-CD8⁺ tumors (HR = 0.33, 95% CI = 0.08–1.23, p = 0.06; Figure 3(C)), but not in low-CD8⁺ tumors (HR = 0.62, 95% CI = 0.26–1.50, p = 0.29; Figure 3(D)).

Multivariate Cox analysis in the high-CD8⁺ subgroup identified tumor site (HR = 0.43, 95% CI: 0.20–0.92, p = 0.03) and macrophage density (HR = 0.79, 95% CI: 0.63–0.98, p = 0.03) as protective factors, whereas high Treg cell density was linked to poorer outcomes (HR = 1.22, 95% CI: 1.05–1.41, p = 0.01) (Figure 3(E), and Supplementary Table S6). Interestingly, univariate analysis within this subgroup did not yield significant associations (Supplementary Table S7), suggesting that the prognostic effect of macrophages and Treg cells emerges only in the context of high CD8⁺ T cell infiltration. No variable reached significance in the low-CD8⁺ group (Figure 3(F), and Supplementary Table S8). These findings underscore the context-dependent interactions between immune subsets in shaping patient prognosis in early-stage CRC.

Validation of laminin a4 association with CD8⁺ T cell and macrophage infiltration

To validate our initial observations, we retrospectively analyzed an independent cohort of 226 patients with stage II CRC, assessing LM α 4 expression alongside infiltration of CD8⁺ T cells, Treg cells (FoxP3⁺) and macrophages (CD68⁺). In this validation cohort, CD8⁺ T cells again represented the predominant tumor-infiltrating immune population, while Tregs the least abundant (Figure 4(A)).

In line with the study cohort, a significant positive correlation was found between LM α 4 z-scores and intratumor densities of CD8⁺ T cells (r = 0.24, p = 0.001; Figure 4(B)) and macrophages (r = 0.17, p = 0.01; Figure 4(C)), but not Treg cells (r = -0.11, p = 0.1; Figure 4(D)). Furthermore, CD8⁺ T cell infiltration positively correlated with macrophage density (r = 0.16, p = 0.02; Figure 4(E)), whereas no association was found with Treg cell density (r = 0.02, p = 0.71; Figure 4(F)). These results confirm the results from the study cohort and reinforce the notion that LM α 4 expression positively influence CD8⁺ T cell and macrophage tumor infiltration, but not Treg cells.

Validation of the prognostic relevance and interplay among immune cell subtypes

ROC analyses were performed to determine optimal prognostic cutoffs for LM α 4 z-scores (\geq 50), CD8⁺ T cells (\geq 20 cells/mm²), Treg cells (>0 cells/mm²), and macrophages (>16 cells/mm²). Kaplan-Meier analyses revealed that high densities of intratumor CD8⁺ T cells (HR = 0.30, 95% CI = 0.14–0.63, p = 0.001; Figure 5(A)) and macrophages (HR = 0.37, 95% CI = 0.20–0.70, p = 0.007; Figure 5(B)) were significantly associated with a reduced risk of relapse, whereas Treg cell infiltration alone had no prognostic impact (HR = 1.20, 95% CI = 0.62–2.32, p = 0.56; Figure 5(C)).

In multivariate Cox regression analyses adjusted for clinical variables (Suppl. Table S9), CD8⁺ T cell density remained an independently protective factor (HR = 0.96, 95% CI = 0.94–0.99, p < 0.005; Figure 5 (D)). Notably, Treg cell density showed a modest but statistically significant association with worse prognosis (HR = 1.07, 95% CI = 1.01–1.13, p = 0.03) in this validation cohort. Nevertheless, only CD8⁺ T cell density reached statistical significance in univariate analysis (HR = 0.96, 95% CI = 0.94–0.99, p < 0.005, for CD8; HR = 1.05, 95% CI = 0.99–1.11, p = 0.07, for Tregs), suggesting that the negative prognostic impact of Treg cells emerges only after adjusting for other clinical and immunological variables.

Stratified Kaplan-Meier analyses further supported this notion. Among tumors with high CD8⁺ T cell infiltration, those with concomitant high Treg cell density exhibited worse outcomes (HR = 5.06, 95% CI = 1.45–14.96, p = 0.02; Figure 6(A)), while this effect was absent in tumors with low-CD8⁺ T cell numbers (HR = 1.96, 95% CI = 0.67–6.47, p = 0.17; Figure 6(B)). Likewise, macrophage-rich tumors within the high-CD8⁺ group were associated with improved prognosis (HR = 0.25, 95% CI = 0.07–0.87, p = 0.04; Figure 6(C)), whereas this benefit was less clear in the low-CD8⁺ group (HR = 0.33, 95% CI = 0.14–0.79, p = 0.05; Figure 6(D)). Multivariate Cox models confirmed the prognostic interactions of Treg cells and macrophages with CD8⁺ T cells in the high-CD8⁺ subgroup (Figure 6(E); Supplementary Table S10), but not in tumors with low CD8⁺ T cell infiltration (Figure 6(F); Supplementary Table S11).

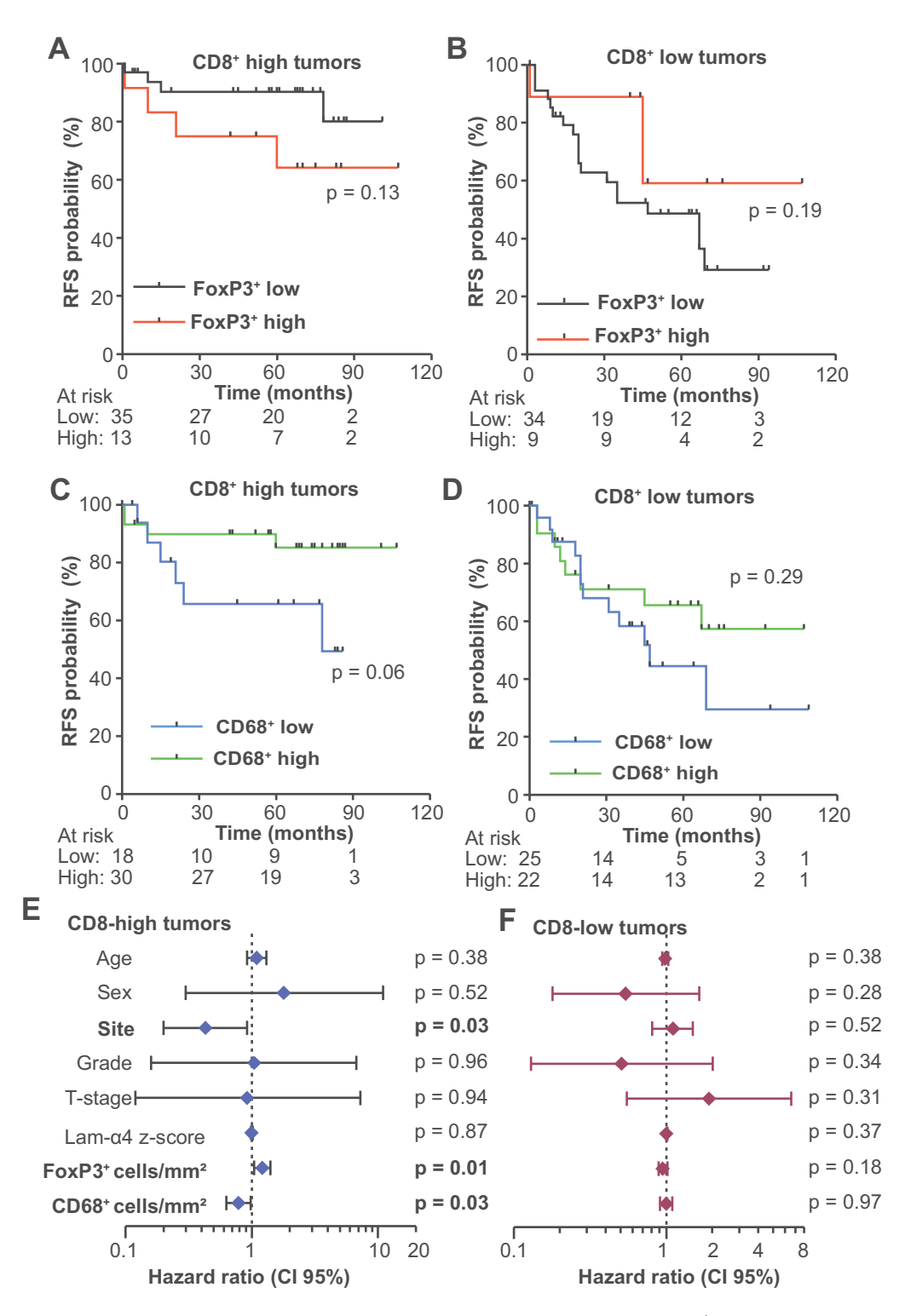


Figure 3. The prognostic significance of Treg cells and macrophages depends on CD8⁺ T cell abundance. (A–D) Kaplan-Meier RFS curves and number of patients at risk in the study cohort, stratified by high or low intratumor CD8⁺ T cell abundance and high or low density of intratumor Treg cells (A, B), or macrophages (C, D). p-values were determined using the log-rank test. (E, F) multivariate Cox regression analysis of clinical and immune parameters in the CRC study cohort, stratified by intratumor CD8⁺ T cell abundance. Hazard ratios and 95% CIs are shown. Additional statistical data are provided in Suppl. Table S6 and Suppl. Table S8.

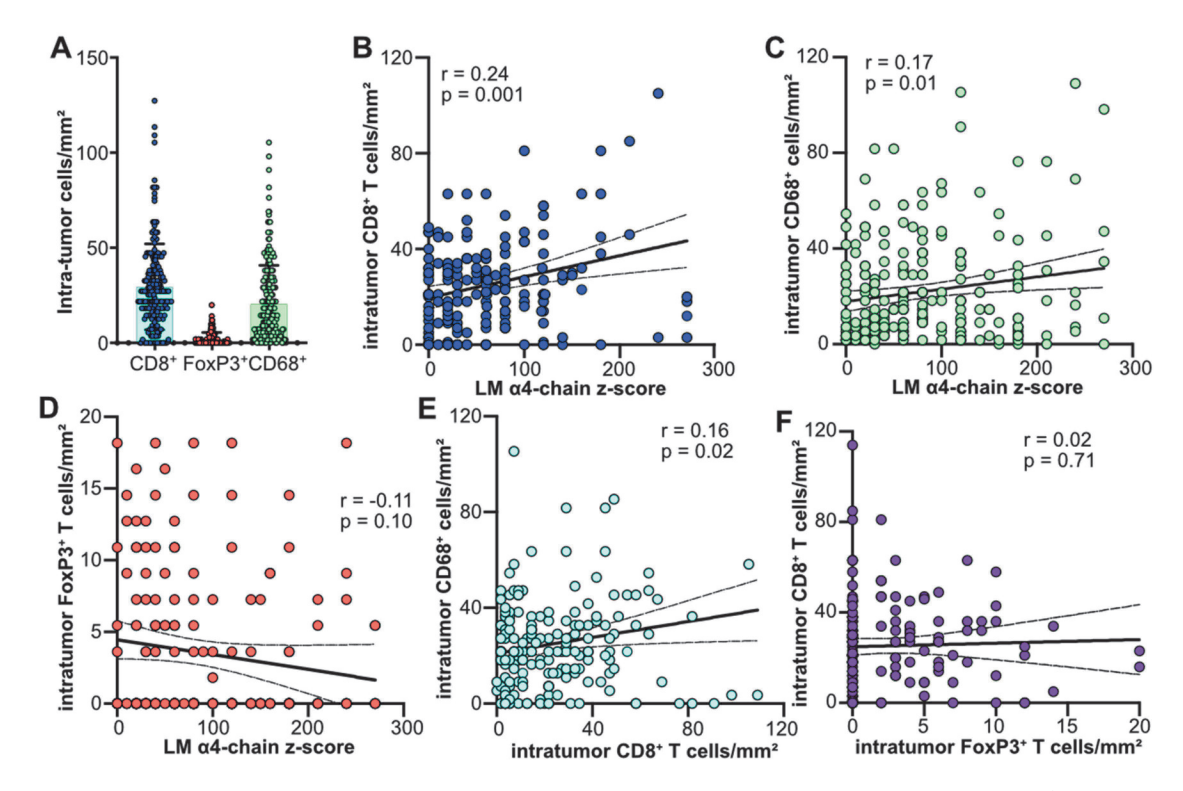


Figure 4. Correlations between LMα4 and immune cell subtypes in the validation cohort. (A) number of immune cells per mm² determined by counting in each TMA (B–D) correlation between the LMα4 z-score and tumor-infiltrating CD8⁺ T cells (B), macrophages (C), and Treg cells (D). (E–F) correlation between intratumor CD8⁺ T cells and macrophages (E) or Treg cells (F). Dotted lines represent 95% confidence intervals. p-values are indicated in the figures. Statistical tests: two-tailed Pearson's correlation coefficient. The regression coefficient and the p-value are indicated in each graph.

Together, these data validate the findings of the initial study cohort and highlight the pivotal role of immune cell cross-regulation between macrophages, CD8⁺ and Tregs cells in shaping recurrence risk early-stage CRC.

The positive correlation between laminin $\alpha 4$ levels and intratumor CD8⁺ T cells and macrophages is independent of clinical stage

To further evaluate the association between LM α 4 and immune cell infiltration, we analyzed the TCGA COAD cohort using TIMER 2.0 to estimate immune composition. Tumors were stratified by clinical stage. In stage I – II tumors, CD8⁺ T cells emerged as the predominant immune population (Figure 7(A)). In line with our previous cohorts, *LAMA4* expression positively correlated with CD8⁺ T cell (r = 0.13, p = 0.03; Figure 7(B)) and macrophage abundance (r = 0.17, p = 0.005; Figure 7(C)), but showed no significant association with Treg cell infiltration (r = 0.01, p = 0.81; Figure 7(D)). Similarly, CD8⁺ T cell density correlated with macrophage levels (r = 0.12, p = 0.03; Supplementary Figure S4A), but not with Treg density (Supplementary Figure S4B).

We then assessed whether these correlations persisted in advanced-stage (III – IV) tumors. TIMER again identified CD8⁺ T cells as the most abundant infiltrating population, followed by macrophages and Tregs (Figure 7(E)). *LAMA4* expression remained significantly correlated with both CD8⁺ T cell (r = 0.29, p < 0.0001; Figure 7(F)) and macrophage infiltration (r = 0.37, p < 0.0001; Figure 7(G)), but not with Treg cells (r = -0.02, p = 0.69; Figure 7(H)). CD8⁺ T cell and macrophage infiltration were strongly correlated (r = 0.72, p < 0.0001; Supplementary Figure S4C), whereas Treg infiltration remained unassociated (r = 0.03, p = 0.61; Supplementary Figure S4D). Collectively, these findings indicate that the positive association between LMα4-chain expression and both CD8⁺ T cell and macrophage density is maintained across different clinical stages.

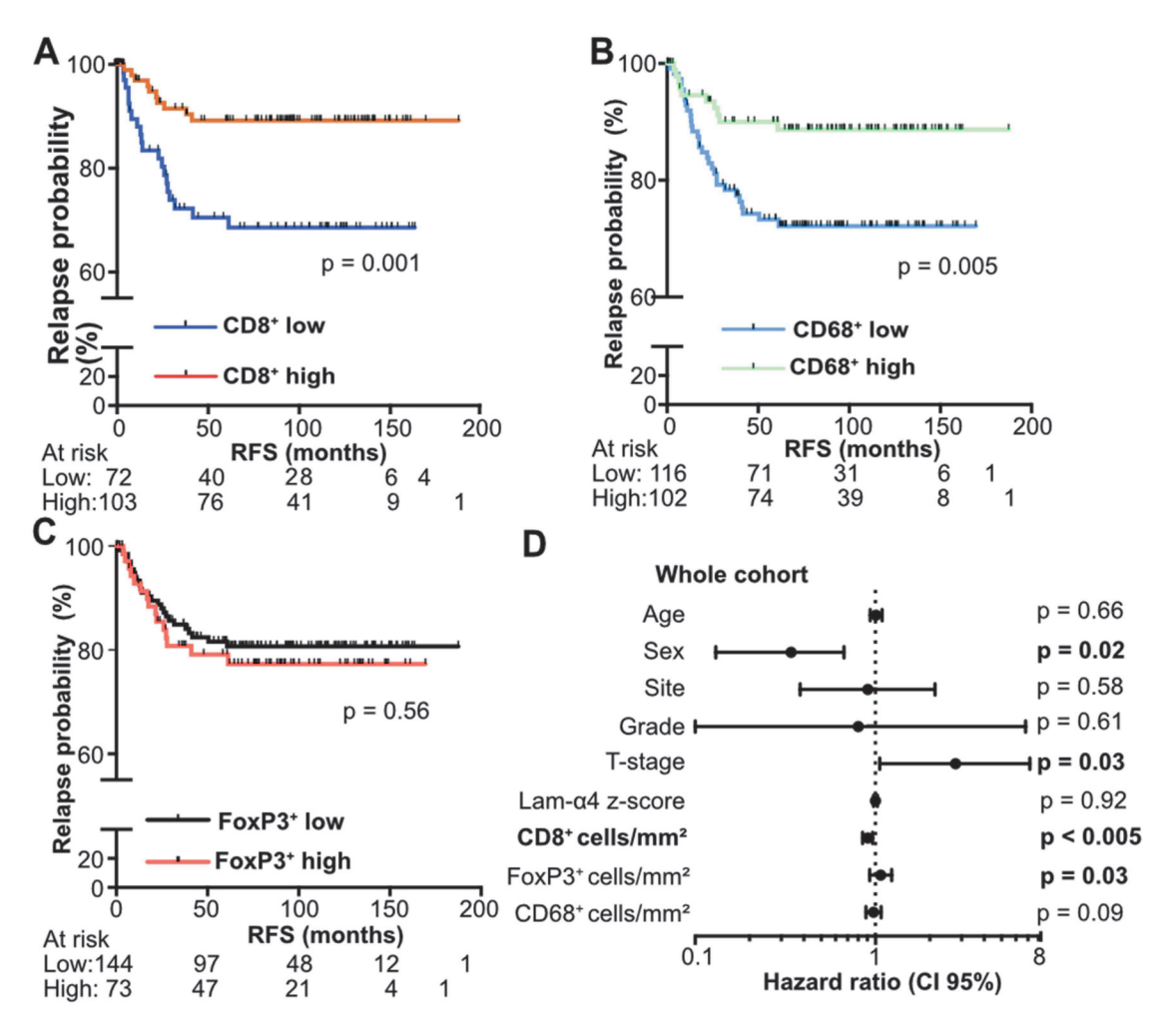


Figure 5. Validation of the predictive impact of immune subtypes in an independent CRC cohort. (A–C) Kaplan-Meier RFS curves and number of patients at risk in the validation cohort, based on groups defined by high or low intratumor abundance of CD8⁺ T cells (A), CD68⁺ macrophages (B), or Treg (FoxP3⁺) cells (C). p-values were determined using the logrank test. (D) multivariate Cox regression analysis of clinical and immune parameters in the CRC validation cohort. The hazard ratio and 95% confidence interval (CI) are shown. Additional data from the correlation analysis are provided in Suppl. Table S9.

We also explored the prognostic significance of immune cell infiltration in the stage I – II COAD cohort. However, data on RFS were unavailable, and only overall survival (OS) was recorded. ROC analysis failed to identify meaningful thresholds to distinguish tumors with high vs. low CD8⁺ T cell infiltration, as the true positive rate increased proportionally with the false positive rate (Supplementary FIgure S5). Similar results were obtained for Treg cells and macrophages (not shown), suggesting limited predictive value of these variables in this dataset.

Unexpectedly, multivariate Cox regression identified both age (HR = 1.06, 95% CI: 1.01–1.11, p = 0.01) and CD8⁺ T cell abundance (HR = 2.66, 95% CI: 1.18–5.98, p = 0.02) as independent predictors of poor OS (Suppl. Table S12). This counterintuitive association between high CD8⁺ T cell density and poor prognosis in the TCGA COAD cohort has been previously reported and linked to distinct tumor mutational profiles. When highly infiltrated tumors were excluded, only age remained a significant poor prognosis predictor in both multivariate (Suppl. Table S13) and univariate analyses (p < 0.005). These observations suggest that this cohort has limited value for prognostic modeling in early-stage CRC.

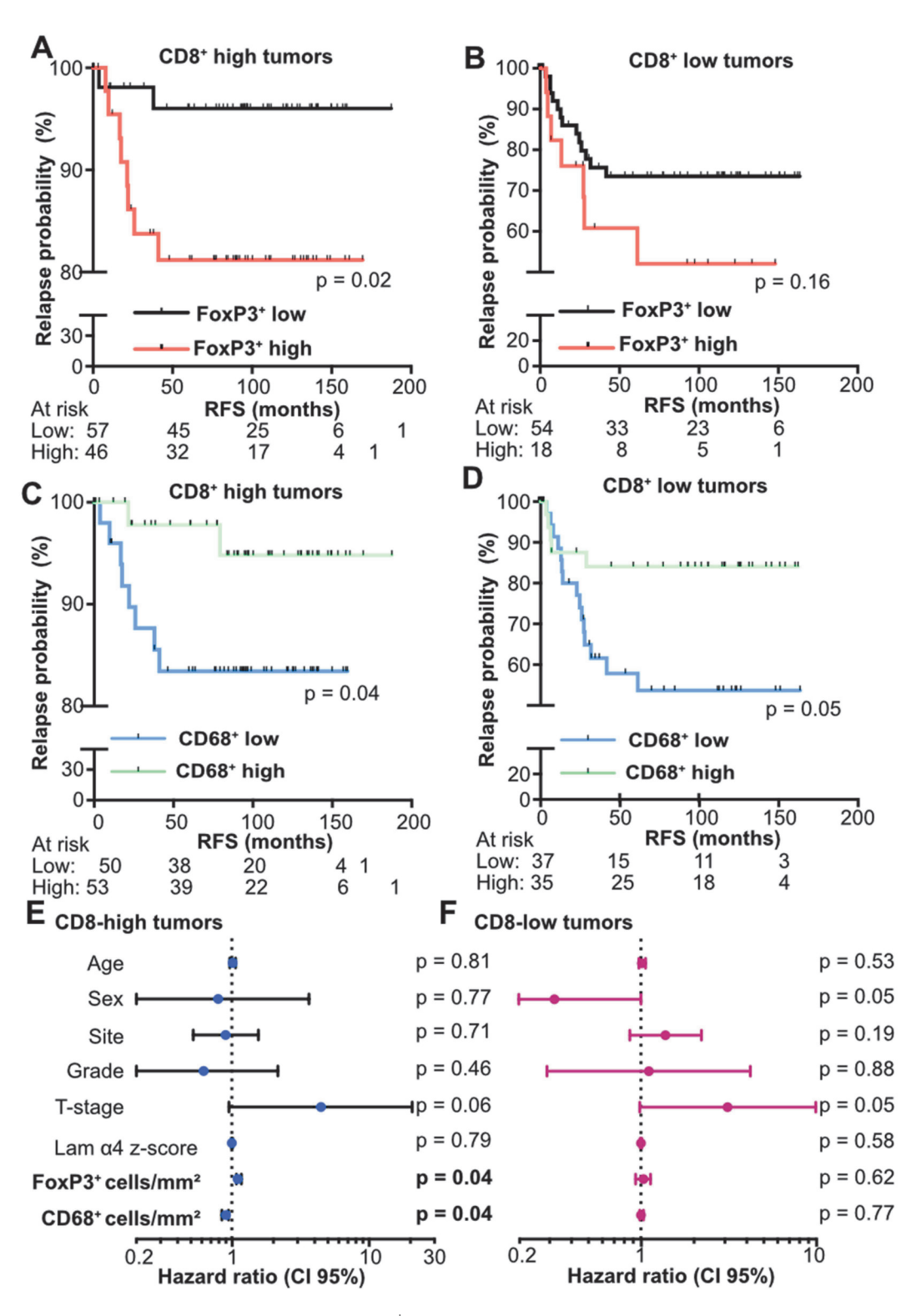


Figure 6. Validation of the interactions between CD8⁺ T cells, macrophages, and Treg cells in predicting the prognosis of early-stage CRC. (A–D) Kaplan-Meier RFS curves and number of patients at risk in the validation cohort, stratified by high or low intratumor CD8⁺ T cell abundance and high or low density of intratumor Treg cells (A, B), or macrophages (C, D). p-values were determined using the log-rank test. (E, F) multivariate Cox regression analysis of clinical and immune parameters in the CRC study cohort, stratified by intratumor CD8⁺ T cell abundance. Hazard ratios and 95% CIs are shown. Additional statistical data are provided in Suppl. Table S10 and Suppl. Table S11.

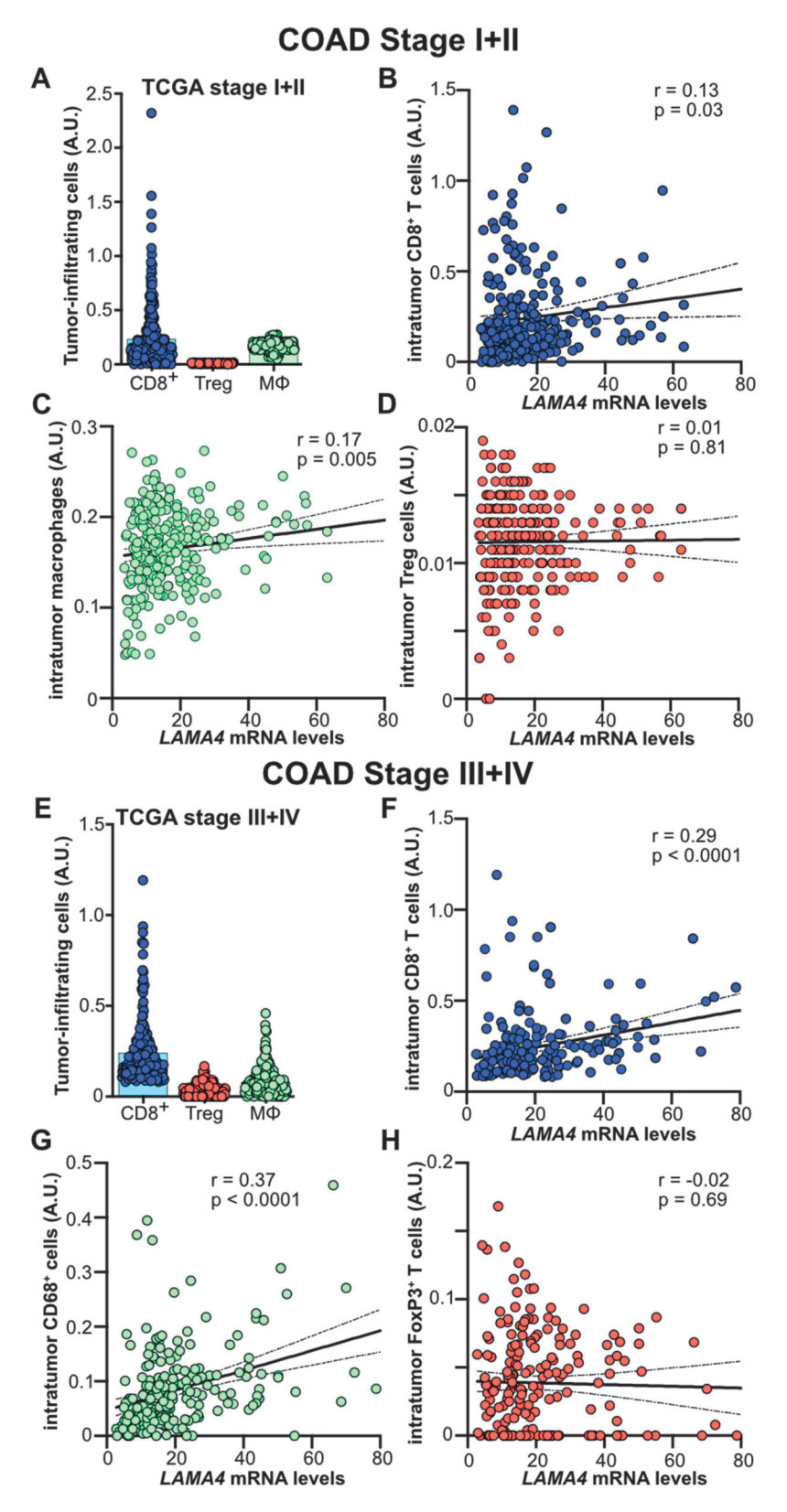


Figure 7. LM α4 expression with CD8⁺ T cell and macrophage infiltration across all clinical stages. (A) estimation of immune cell subtypes using TIMER from the whole transcriptome data of the COAD cohort stage I/II. (B–D) correlation analyses of *LAMA4* mRNA levels with intratumor CD8⁺ T cells (B), macrophages (C) and Treg cells (D) in this cohort. (E) estimation of immune cell subtypes using TIMER from whole transcriptome data in the COAD cohort stratified by stages III and IV. (F–H) correlation analyses of *LAMA4* mRNA levels with intratumor CD8⁺ T cells (B), macrophages (C) and Treg cells (D) in this cohort. Dotted lines represent 95% confidence intervals. p-values are indicated in the figures. Statistical test: two-tailed Pearson's correlation coefficient.

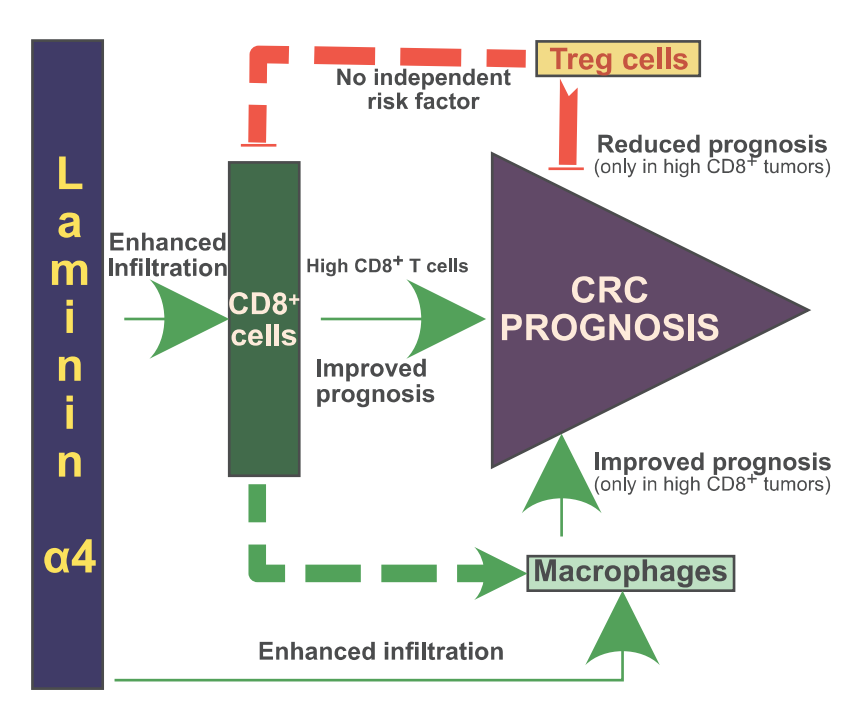


Figure 8. Proposed model of LMα4-chain interactions with immune cells and their impact on prognosis. LM α4-chain expression is positively associated with CD8⁺ T cell and macrophage infiltration (green line), but does not affect intratumor Treg cell accumulation. Our findings suggest that CD8⁺ T cells play a central role in prognosis by not only exerting direct anti-tumor effects but also influencing macrophage activity. Treg cells have a limited impact on recurrence prediction by reducing the prognostic significance of CD8⁺ T cells. Green lines indicate positive prognostic effects, while dotted red lines denote negative influences.

Discussion

The tumor immune microenvironment, particularly cytotoxic CD8 $^+$ T lymphocytes, plays a pivotal influence in CRC progression. However, the molecular cues governing immune cell infiltration remain poorly understood. Here, we examined the relationship between vascular LM α 4-chain expression, intratumor infiltration by CD8 $^+$ T cells, Treg cells and macrophages, as well as its prognostic significance in early-stage CRC.

LM α 4-chain may have a site-specific, dual role in cancer progression. In glioblastoma, breast, oral and pancreatic cancers, high LM α 4-chain expression in cancer cells promotes tumor growth and stemness. ⁴¹ In contrast, in gastric and colorectal cancers, LM α 4 upregulation within the stroma is linked to enhanced immune infiltration and improved clinical outcomes. ^{29,42} Beyond cancer, LM α 4 facilitates diapedesis of various immune cell subtypes, including T cells, monocytes, neutrophils and dendritic cells, into inflamed tissues. ^{28,43–46} LM α 4 seems to mediate Treg cell homing into tolerogenic lymph nodes inducing their transmigration through high endothelial venules. ²⁸ Our study reveals a more selective and complex role for LM α 4 in CRC. Across three independent cohorts, LM α 4 expression positively correlated with intratumor CD8⁺ T cells and macrophages, but not with FoxP3⁺ Treg cells. This pattern held true across early- and latestage disease, suggesting a consistent role for LM α 4 in shaping immune composition within the TME.

The lack of correlation between LM α 4-chain expression and Treg cell infiltration suggests distinct diapedesis mechanisms for CD8⁺ and Treg cells. Since cell migration relies on substrate adhesion, ⁴⁷ the divergence between CD8⁺ and Treg cell infiltration may stem from differences in their laminin receptor expression pattern. Given its unique structure, LM α 4-chain binds with low affinity only α 6 β 1 (also known as VLA-6) and α 7 β 1 integrins, ⁴⁸ which are similarly expressed in splenic CD8⁺ T cells and thymus-derived Treg cells. ⁴⁹ The contribution of non-integrin laminin receptors to T cell function remains insufficiently characterized; consequently their potential involvement in the differential adhesion of CD8⁺ and Treg cells to LM α 4 is an open possibility. Moreover, adhesion to LM α 4 alone is unlikely to fully determine migratory behavior²⁷; other vascular features, such as stiffness, permeability, or chemokine gradients, may differentially guide effector and regulatory T cells. ^{21,24}

We also examined the prognostic relevance of immune infiltration in our primary and validation cohorts. $CD8^+$ T cell and macrophage abundance -both positively associated with $LM\alpha4$ - were linked to reduced relapse risk. Multivariate analysis confirmed $CD8^+$ T cell density as an independent protective factor. Notably, $CD8^+$ T cell infiltration in the TCGA-COAD dataset paradoxically correlated with poor prognosis, likely reflecting a distinct subset of highly infiltrated tumors with unique molecular profiles. After excluding these outliers, age was the sole variable associated with prognosis, possibly reflecting wide age variation (30–90 years) and survival bias in older patients. These limitations, alongside the lack of relapse-specific endpoints, diminish the utility of the TCGA-COAD cohort for prognostic biomarker discovery in early-stage CRC.

Another unexpected finding was the lack of prognostic significance for Treg cells in our cohorts. Despite conflicting results¹⁰ linking Treg cell infiltration to both favorable^{11–13,50} and poor^{14,50} CRC outcomes, Kaplan-Meier analyses showed near-identical RFS curves for tumors with high *vs.* low Treg cells. However, when stratified by CD8⁺ T cell abundance, high FoxP3⁺ Treg density was associated with shorter RFS, supporting a model in which intratumor Treg cells suppress CD8⁺ T cell-mediated tumor immunity. Prior spatial studies using Voronoi tessellation have shown that close Treg-CD8⁺ T cells proximity predicts poor prognosis in 18% of CRC tumors.⁵⁰ Nonetheless, multivariate analysis after CD8⁺ stratification revealed prognostic significance for Treg cell density, suggesting that Tregs do not act independently but modulate the prognostic value of effector T cells.

Likewise, macrophage infiltration has a strong impact on CRC prognosis depending on CD8⁺ T cell density. In multivariate Cox models, macrophage density significantly predicted outcome only within CD8⁺-high tumors. These data support a cooperative model in which macrophages require effector T cell-derived cues to adopt tumor-suppressive functions. Macrophage polarization is highly plastic and shaped by microenvironmental inputs such as metabolic stress, tumor-derived exosomes, and immune cytokines. Cytokines from immunosuppressive T cells, such as IL-13, IL-10 or TGF- β , skew macrophages toward a pro-tumor phenotype, whereas CD8⁺ T cell-derived type I and type II interferons, drive anti-tumor polarization. Given the positive correlation between CD8⁺ T cells and macrophages, we speculate that a high density of activated CD8⁺ T cells enhances anti-tumor macrophage polarization *via* cytokine signaling. LM α 4 may co-regulate the transmigration and cooperative function of these cell types within the TME.

In summary, our findings support a model (Figure 8) in which LM α 4 expression promotes the coordinated infiltration of CD8⁺ T cells and macrophages, enhancing anti-tumor immunity and reducing recurrence risk in early-stage CRC. CD8⁺ T cells emerge as central regulators, exerting direct cytotoxicity and orchestrating macrophage polarization. Conversely, Treg cells do not independently influence prognosis but may attenuate the protective effects of CD8⁺ T cells when present at high density. Further studies are needed to validate this model in larger, relapse-annotated CRC cohorts and to elucidate the molecular determinants of α 4-containing laminins-guided immune cell diapedesis.

Acknowledgments

We are deeply grateful to patients for their participation and contribution to this study. We also thank for their support and constructive comments to the Mañes' lab members, and the pathologists and technicians at the Hospital Clínico San Carlos.

Disclosure statement

No potential conflict of interest was reported by the author(s).

Funding

The work was funded by Spanish Ministry of Science, Innovation and Universities (MICIU/AEI/10.13039/501100011033) under grants PID2020-116303RB-I00 (SM), PID2023-147125OB-I00 (SM), and CEX2023-001386-S (Severo Ochoa Programme); and the Asociación Española Contra el Cáncer Foundation under grant PRYGN211240MAÑE (SM). Elena Nonnast is supported by a predoctoral fellowship from the Formación de Personal Investigador (PRE2021-097603), from the Spanish Ministry of Science and Innovation with the support of the EU European Social Fund. TP is supported in part by the Comunidad de Madrid under grant P2022/BMD-7321/MITIC-CM. SM belongs to the Spanish National Research Council (CSIC)'s Cancer Hub; Fundación Científica



Asociación Española Contra el Cáncer [PRYGN211240MAÑE]; Ministerio de Ciencia e Innovación [PID2020-116303RB-I00, PID2023-147125OB-I00,]; Ministerio de Ciencia e Innovación [PRE2021-097603]; Ministerio de Ciencia e Innovación [CEX2023-001386-S].

ORCID

Santos Mañes (b) http://orcid.org/0000-0001-8023-957X

Authors contribution

Conceptualization: SM, MJF-A; Methodology: EM, EN, MJF-A, MPDS, TP, CÓSS; Investigation and Formal analysis: EM, EN, MJF-A, MPDS, TP, CÓSS; Data Curation: EN, MJF-A, TP, SM; Writing – Original draft: SM; Writing – Review & Editing: EM, EN, MJF-A, TP, MPDS, CÓSS; Visualization: SM, EN; Funding acquisition: SM

Data availability statement

Authors agree to make data and materials supporting results or analyses presented in this paper available upon reasonable request.

Ethics approval and consent to participate

This study was approved by the Ethical Review Board of Hospital Fundación Jiménez Díaz (Act number 17/24; study cohort) and of Hospital Infanta Leonor (004–22; validation cohort). Appropriate informed consent was obtained from all patients and no personal data were recorded. Fundamental ethical principles and rights promoted by Spain (LOPD 15/1999) and the European Union (200/C364/01) were followed.

References

- 1. Dunne PD, Arends MJ. Molecular pathological classification of colorectal cancer-an update. Virchows Arch. 2024;484(2):273–285. doi: 10.1007/S00428-024-03746-3.
- 2. Paz-Cabezas M, Calvo-López T, Romera-Lopez A, Tabas-Madrid D, Ogando J, Fernández-Aceñero MJ, Sastre J, Pascual-Montano A, Mañes S, Díaz-Rubio E, et al. Molecular classification of colorectal cancer by microRNA profiling: correlation with the consensus molecular subtypes (CMS) and validation of miR-30b targets. Cancers (Basel). 2022;14(21):5175. doi: 10.3390/CANCERS14215175.
- 3. de Back TR, Wu T, Schafrat PJ, Ten Hoorn S, Tan M, He L, van Hooff SR, Koster J, Nijman LE, Vink GR, et al. A consensus molecular subtypes classification strategy for clinical colorectal cancer tissues. Life Sci Alliance. 2024;7(8):e202402730. doi: 10.26508/LSA.202402730.
- 4. Weitz J, Koch M, Debus J, Höhler T, Galle PR, Büchler MW. Colorectal cancer. Lancet. 2005;365(9454):153–165. doi: 10.1016/S0140-6736(05)17706-X.
- 5. Kuznetsova O, Fedyanin M, Zavalishina L, Moskvina L, Kuznetsova O, Lebedeva A, Tryakin A, Kireeva G, Borshchev G, Tjulandin S, et al. Prognostic and predictive role of immune microenvironment in colorectal cancer. World J Gastrointest Oncol. 2024;16(3):643–652. doi: 10.4251/WJGO.V16.I3.643.
- 6. Kim JK, Chen CT, Keshinro A, Khan A, Firat C, Vanderbilt C, Segal N, Stadler Z, Shia J, Balachandran VP, et al. Intratumoral T-cell repertoires in DNA mismatch repair-proficient and -deficient colon tumors containing high or low numbers of tumor-infiltrating lymphocytes. Oncoimmunology. 2022;11(1):2054757. doi: 10.1080/2162402X.2022.2054757.
- 7. Hijazi A, Antoniotti C, Cremolini C, Galon J. Light on life: immunoscore immune-checkpoint, a predictor of immunotherapy response. Oncoimmunology. 2023;12(1):2243169. doi: 10.1080/2162402X.2023.2243169.
- 8. Pagès F, Mlecnik B, Marliot F, Bindea G, Ou FS, Bifulco C, Lugli A, Zlobec I, Rau TT, Berger MD, et al. International validation of the consensus immunoscore for the classification of colon cancer: a prognostic and accuracy study. Lancet. 2018;391(10135):2128–2139. doi: 10.1016/S0140-6736(18)30789-X.
- 9. Tse BCY, Bergamin S, Steffen P, Hruby G, Pavlakis N, Clarke SJ, Evans J, Engel A, Kneebone A, Molloy MP. CD11c+ and IRF8+ cell densities in rectal cancer biopsies predict outcomes of neoadjuvant chemoradiotherapy. Oncoimmunology. 2023;12(1):2238506. doi: 10.1080/2162402X.2023.2238506.
- Aristin Revilla S, Kranenburg O, Coffer PJ. Colorectal cancer-infiltrating regulatory T cells: functional heterogeneity, metabolic adaptation, and therapeutic targeting. Front Immunol. 2022;13:903564. doi: 10.3389/FIMMU. 2022.903564.



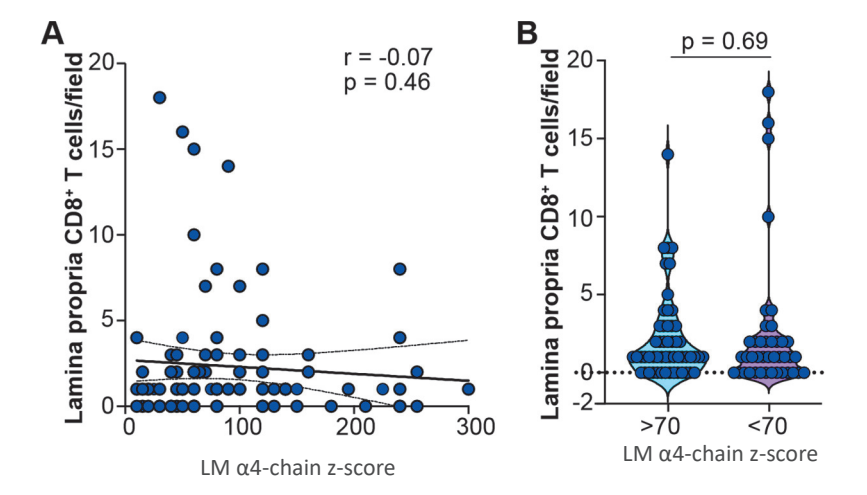
- 11. Frey DM, Droeser RA, Viehl CT, Zlobec I, Lugli A, Zingg U, Oertli D, Kettelhack C, Terracciano L, Tornillo L. High frequency of tumor-infiltrating FOXP3+ regulatory T cells predicts improved survival in mismatch repair-proficient colorectal cancer patients. Intl J Cancer. 2010;126(11):2635–2643. doi: 10.1002/IJC.24989.
- 12. Sinicrope FA, Rego RL, Ansell SM, Knutson KL, Foster NR, Sargent DJ. Intraepithelial effector (CD3+)/regulatory (FoxP3+) T-cell ratio predicts a clinical outcome of human colon carcinoma. Gastroenterology. 2009;137 (4):1270–1279. doi: 10.1053/J.GASTRO.2009.06.053.
- 13. Salama P, Phillips M, Grieu F, Morris M, Zeps N, Joseph D, Platell C, Iacopetta B. Tumor-infiltrating FOXP3+ T regulatory cells show strong prognostic significance in colorectal cancer. J Clin Oncol. 2009;27(2):186–192. doi: 10.1200/JCO.2008.18.7229.
- 14. Li Q, Chu Y, Yao Y, Song Q. A Treg-related riskscore model may improve the prognosis evaluation of colorectal cancer. J Gene Med. 2024;26(2). doi: 10.1002/JGM.3668.
- 15. Wu X, Zhou Z, Cao Q, Chen Y, Gong J, Zhang Q, Qiang Y, Lu Y, Cao G. Reprogramming of Treg cells in the inflammatory microenvironment during immunotherapy: a literature review. Front Immunol. 2023;14:1268188. doi: 10.3389/FIMMU.2023.1268188.
- 16. Saito T, Nishikawa H, Wada H, Nagano Y, Sugiyama D, Atarashi K, Maeda Y, Hamaguchi M, Ohkura N, Sato E, et al. Two FOXP3(+)CD4(+) T cell subpopulations distinctly control the prognosis of colorectal cancers. Nat Med. 2016;22(6):679-684. doi: 10.1038/NM.4086.
- 17. Hou S, Zhao Y, Chen J, Lin Y, Qi X. Tumor-associated macrophages in colorectal cancer metastasis: molecular insights and translational perspectives. J Transl Med. 2024;22(1):62. doi: 10.1186/S12967-024-04856-X.
- 18. Mira E, Carmona-Rodríguez L, Tardáguila M, Azcoitia I, González-Martín A, Almonacid L, Casas J, Fabriás G, Mañes S. A lovastatin-elicited genetic program inhibits M2 macrophage polarization and enhances T cell infiltration into spontaneous mouse mammary tumors. Oncotarget. 2013;4(12):2288-2301. doi: 10.18632/ ONCOTARGET.1376.
- 19. Li J, Li L, Li Y, Long Y, Zhao Q, Ouyang Y, Bao W, Gong K. Tumor-associated macrophage infiltration and prognosis in colorectal cancer: systematic review and meta-analysis. Int J Colorectal Dis. 2020;35(7):1203–1210. doi: 10.1007/S00384-020-03593-Z.
- 20. Nagorsen D, Voigt S, Berg E, Stein H, Thiel E, Loddenkemper C. Tumor-infiltrating macrophages and dendritic cells in human colorectal cancer: relation to local regulatory T cells, systemic T-cell response against tumor-associated antigens and survival. J Transl Med. 2007;5(1):1-8. doi: 10.1186/1479-5876-5-62.
- 21. Lacalle RA, Blanco R, Carmona-Rodríguez L, Martín-Leal A, Mira E, Mañes S. Chemokine receptor signaling and the hallmarks of cancer. Int Rev Cell Mol Biol. 2017;331:181-244. doi: 10.1016/bs.ircmb.2016.09.011.
- 22. Jayadev R, Sherwood DR. Basement membranes. Curr Biol. 2017;27(6):R207-R211. doi: 10.1016/J.CUB.2017.02.006.
- 23. Aumailley M, Bruckner-Tuderman L, Carter WG, Deutzmann R, Edgar D, Ekblom P, Engel J, Engvall E, Hohenester E, Jones JCR, et al. A simplified laminin nomenclature. Matrix Biol. 2005;24(5):326-332. doi: 10. 1016/J.MATBIO.2005.05.006.
- 24. Nonnast E, Mira E, Mañes S. Biomechanical properties of laminins and their impact on cancer progression. Biochim Biophys Acta Rev Cancer. 2024;1879(6):189181. doi: 10.1016/J.BBCAN.2024.189181.
- 25. Yousif LF, Di Russo J, Sorokin L. Laminin isoforms in endothelial and perivascular basement membranes. Cell Adh Migr. 2013;7(1):101–110. doi: 10.4161/cam.22680.
- 26. Martínez-Rey D, Carmona-Rodríguez L, Fernández-Aceñero MJ, Mira E, Mañes S. Extracellular superoxide dismutase, the endothelial basement membrane, and the WNT pathway: new players in vascular normalization and tumor infiltration by T-Cells. Front Immunol. 2020;11(Oct 30):579552. doi: 10.3389/FIMMU.2020.579552 .
- 27. Song J, Zhang X, Buscher K, Wang Y, Wang H, Di Russo J, Li L, Lutke-Enking S, Zarbock A, Stadtmann A, et al. Endothelial basement membrane laminin 511 contributes to endothelial junctional tightness and thereby inhibits leukocyte transmigration. Cell Rep. 2017;18(5):1256-1269. doi: 10.1016/j.celrep.2016.12.092.
- 28. Warren KJ, Iwami D, Harris DG, Bromberg JS, Burrell BE. Laminins affect T cell trafficking and allograft fate. J Clin Invest. 2014;124(5):2204-2218. doi: 10.1172/JCI73683.
- 29. Carmona-Rodríguez L, Martínez-Rey D, Fernández-Aceñero MJ, González-Martín A, Paz-Cabezas M, Rodríguez-Rodríguez N, Pérez-Villamil B, Sáez ME, Díaz-Rubio E, Mira E, et al. SOD3 induces a HIF-2αdependent program in endothelial cells that provides a selective signal for tumor infiltration by T cells. J Immunother Cancer. 2020;8(1):e000432. doi: 10.1136/JITC-2019-000432.
- 30. Carmona-Rodríguez L, Martínez-Rey D, Martín-González P, Franch M, Sorokin L, Mira E, Mañes S. Superoxide dismutase-3 downregulates laminin a5 expression in tumor endothelial cells via the inhibition of nuclear factor kappa B signaling. Cancers (Basel). 2022;14(5):1226. doi: 10.3390/cancers14051226.
- 31. Labianca R, Nordlinger B, Beretta GD, Mosconi S, Mandala M, Cervantes A, Arnold D. Early colon cancer: ESMO clinical practice guidelines for diagnosis, treatment and follow-up. Ann Oncol. 2013;24(6):vi64-72. doi: 10.1093/annonc/mdt354.
- 32. Ryu HS, Kim J, Park YR, Cho EH, Choo JM, Kim JS, Baek SJ, Kwak JM. Recurrence patterns and risk factors after curative resection for colorectal cancer: insights for postoperative surveillance strategies. Cancers (Basel). 2023;15(24):5791. doi: 10.3390/CANCERS15245791.



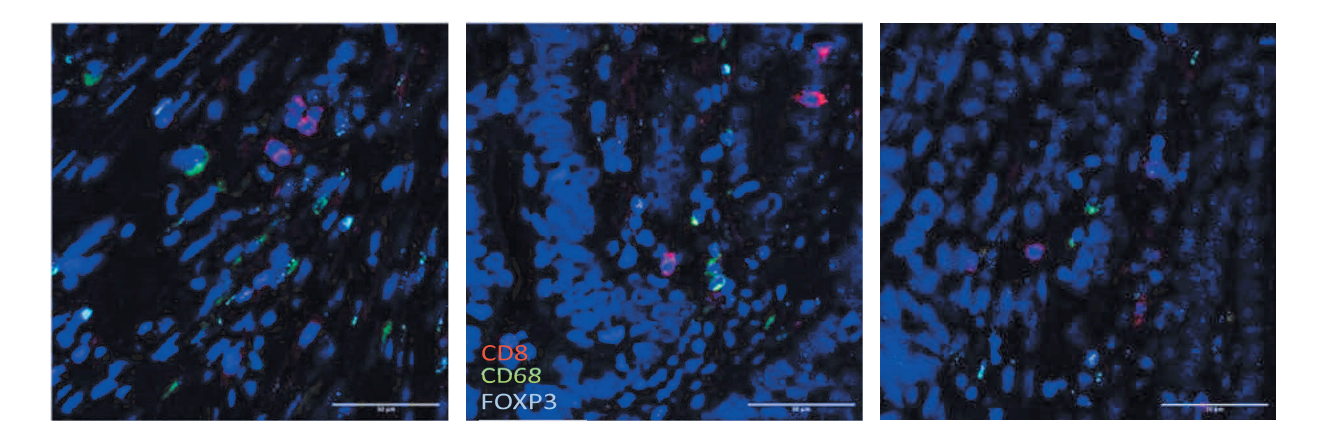
- 33. Neary E, Ibrahim T, Verschoor CP, Zhang L, Patel SV, Chadi SA, Caycedo-Marulanda A. A systematic review and meta-analysis of oncological outcomes with transanal total mesorectal excision for rectal cancer. Colorectal Disease. 2024;26(5):837–850. doi: 10.1111/CODI.16982.
- 34. Vivian J, Rao AA, Nothaft FA, Ketchum C, Armstrong J, Novak A, Pfeil J, Narkizian J, Deran AD, Musselman-Brown A, et al. Toil enables reproducible, open source, big biomedical data analyses. Nat Biotechnol. 2017;35 (4):314–316. doi: 10.1038/nbt.3772.
- 35. Li T, Fu J, Zeng Z, Cohen D, Li J, Chen Q, Li B, Liu XS. TIMER2.0 for analysis of tumor-infiltrating immune cells. Nucleic Acids Res. 2020;48(W1):W509–W514. doi: 10.1093/NAR/GKAA407.
- 36. Lánczky A, Győrffy B. Web-based survival analysis tool tailored for medical research (KMplot): development and implementation. J Med Internet Res. 2021;23(7):e27633. doi: 10.2196/27633.
- 37. McCarty J, Miller KS, Cox LS, Konrath EB, McCarty J. Estrogen receptor analyses. Correlation of biochemical and immunohistochemical methods using monoclonal antireceptor antibodies. Arch Pathol Lab Med. 1985;109 (8):716–721.
- 38. Wang F, Lu S, Cao D, Qian J, Li C, Zhang R, Wang F, Wu M, Liu Y, Pan Z, et al. Prognostic and predictive value of immunoscore and its correlation with ctDNA in stage II colorectal cancer. Oncoimmunology. 2023;12 (1):2161167. doi: 10.1080/2162402X.2022.2161167.
- 39. Eriksen AC, Sorensen FB, Lindebjerg J, Hager H, depont Christensen R, Kjaer-Frifeldt S, Hansen TF. The prognostic value of tumor-infiltrating lymphocytes in stage II colon cancer. A nationwide population-based study. Transl Oncol. 2018;11(4):979–987. doi: 10.1016/j.tranon.2018.03.008.
- 40. Campana LG, Mansoor W, Hill J, Macutkiewicz C, Curran F, Donnelly D, Hornung B, Charleston P, Bristow R, Lord GM, et al. T-Cell infiltration and clonality may identify distinct survival groups in colorectal cancer: development and validation of a prognostic model based on the cancer genome atlas (TCGA) and clinical proteomic tumor analysis consortium (CPTAC). Cancers (Basel). 2022;14(23):5883. doi: 10.3390/CANCERS14235883.
- 41. Nonnast E, Mira E, Mañes S. The role of laminins in cancer pathobiology: a comprehensive review. J Transl Med. 2025;23(1):83. doi: 10.1186/s12967-025-06079-0.
- 42. Wang M, Li C, Liu Y, Wang Z, De Vita A. Effect of LAMA4 on prognosis and its correlation with immune infiltration in gastric cancer. Biomed Res Int. 2021;2021(1):6428873. doi: 10.1155/2021/6428873.
- 43. Zegeye MM, Matic L, Lengquist M, Hayderi A, Grenegård M, Hedin U, Sirsjö A, Ljungberg LU, Kumawat AK. Interleukin-6 trans-signaling induced laminin switch contributes to reduced trans-endothelial migration of granulocytic cells. Atherosclerosis. 2023;371:41–53. doi: 10.1016/J.ATHEROSCLEROSIS.2023.03.010.
- 44. Thyboll J, Kortesmaa J, Cao R, Soininen R, Wang L, Iivanainen A, Sorokin L, Risling M, Cao Y, Tryggvason K. Deletion of the laminin alpha4 chain leads to impaired microvessel maturation. Mol Cell Biol. 2002;22 (4):1194–1202. doi: 10.1128/mcb.22.4.1194-1202.2002.
- 45. Wu C, Ivars F, Anderson P, Hallmann R, Vestweber D, Nilsson P, Robenek H, Tryggvason K, Song J, Korpos E, et al. Endothelial basement membrane laminin alpha5 selectively inhibits T lymphocyte extravasation into the brain. Nat Med. 2009;15(5):519–527. doi: 10.1038/nm.1957.
- 46. Kenne E, Soehnlein O, Genove G, Rotzius P, Eriksson EE, Lindbom L. Immune cell recruitment to inflammatory loci is impaired in mice deficient in basement membrane protein laminin alpha4. J Leukoc Biol. 2010;88 (3):523–528. doi: 10.1189/jlb.0110043.
- 47. Mañes S, Mira E, Gómez-Moutón C, Lacalle RA, Martínez-A C. Cells on the move: a dialogue between polarization and motility. IUBMB Life. 2000;49(2):89–96. doi: 10.1080/15216540050022386.
- 48. Nishiuchi R, Takagi J, Hayashi M, Ido H, Yagi Y, Sanzen N, Tsuji T, Yamada M, Sekiguchi K. Ligand-binding specificities of laminin-binding integrins: a comprehensive survey of laminin-integrin interactions using recombinant alpha3beta1, alpha6beta1, alpha7beta1 and alpha6beta4 integrins. Matrix Biol. 2006;25(3):189–197. doi: 10.1016/j.matbio.2005.12.001.
- 49. Bertoni A, Alabiso O, Galetto AS, Baldanzi G. Integrins in T cell physiology. Int J Mol Sci. 2018;19(2):485. doi: 10.3390/IJMS19020485.
- 50. Bergsland CH, Jeanmougin M, Moosavi SH, Svindland A, Bruun J, Nesbakken A, Sveen A, Lothe RA. Spatial analysis and CD25-expression identify regulatory T cells as predictors of a poor prognosis in colorectal cancer. Mod Pathol. 2022;35(9):1236–1246. doi: 10.1038/s41379-022-01086-8.
- 51. Yin T, Li X, Li Y, Zang X, Liu L, Du M. Macrophage plasticity and function in cancer and pregnancy. Front Immunol. 2023;14:1333549. doi: 10.3389/fimmu.2023.1333549.
- 52. Nicolini A, Ferrari P. Involvement of tumor immune microenvironment metabolic reprogramming in colorectal cancer progression, immune escape, and response to immunotherapy. Front Immunol. 2024;15:1353787. doi: 10. 3389/FIMMU.2024.1353787.
- 53. Ramil CP, Xiang H, Zhang P, Cronin A, Cabral L, Yin Z, Hai J, Wang H, Ruprecht B, Jia Y, et al. Extracellular vesicles released by cancer-associated fibroblast-induced myeloid-derived suppressor cells inhibit T-cell function. Oncoimmunology. 2024;13(1):2300882. doi: 10.1080/2162402X.2023.2300882.

Supplementary information:

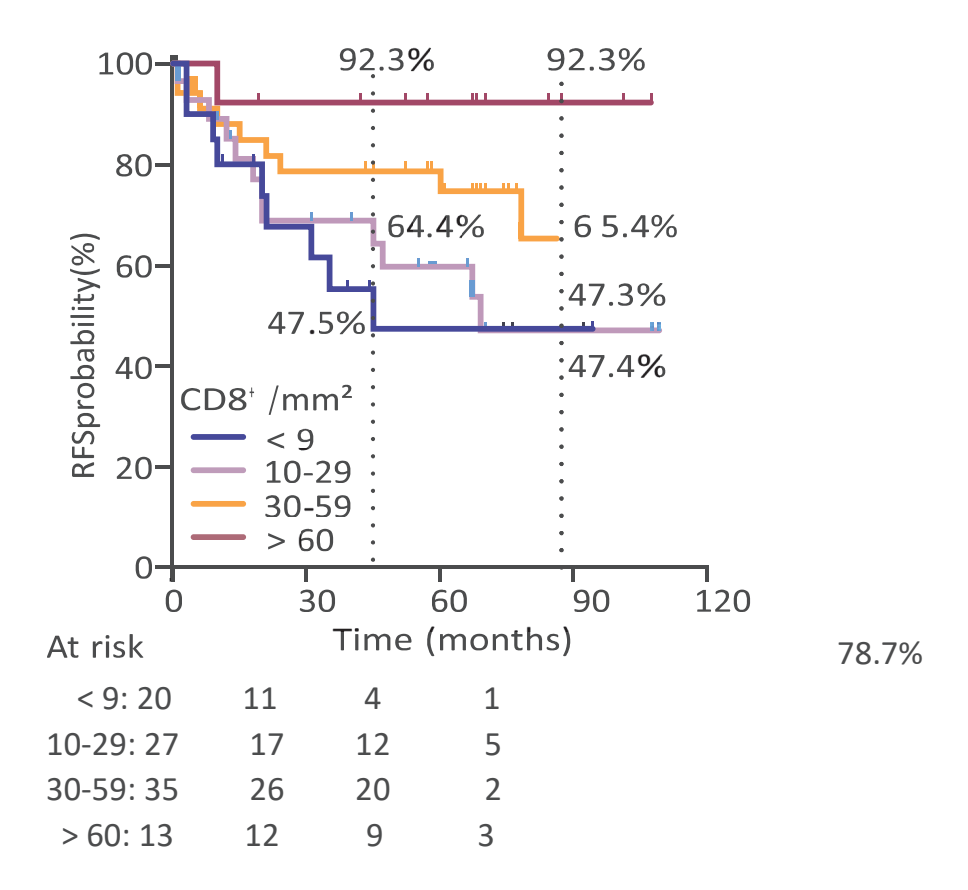
- Supplementary Figures S1-S5
- Supplementary Tables S1-S13



Suppl. Figure S1. LM α 4-chain levels do not correlate with CD8⁺ T cell density in the lamina propria. A) Correlation between LM α 4-chain z-score and CD8⁺ T cell density in the lamina propria. Two-tailed Pearson's correlation coefficient. B) Violin plots with individual data points showing the number and distribution of lamina propria CD8⁺ T cells (cells/ mm²) in tumors with high (z-score > 70) or low (z-score < 70) LM α 4-chain expression. Two-tailed Student's *t*-test.



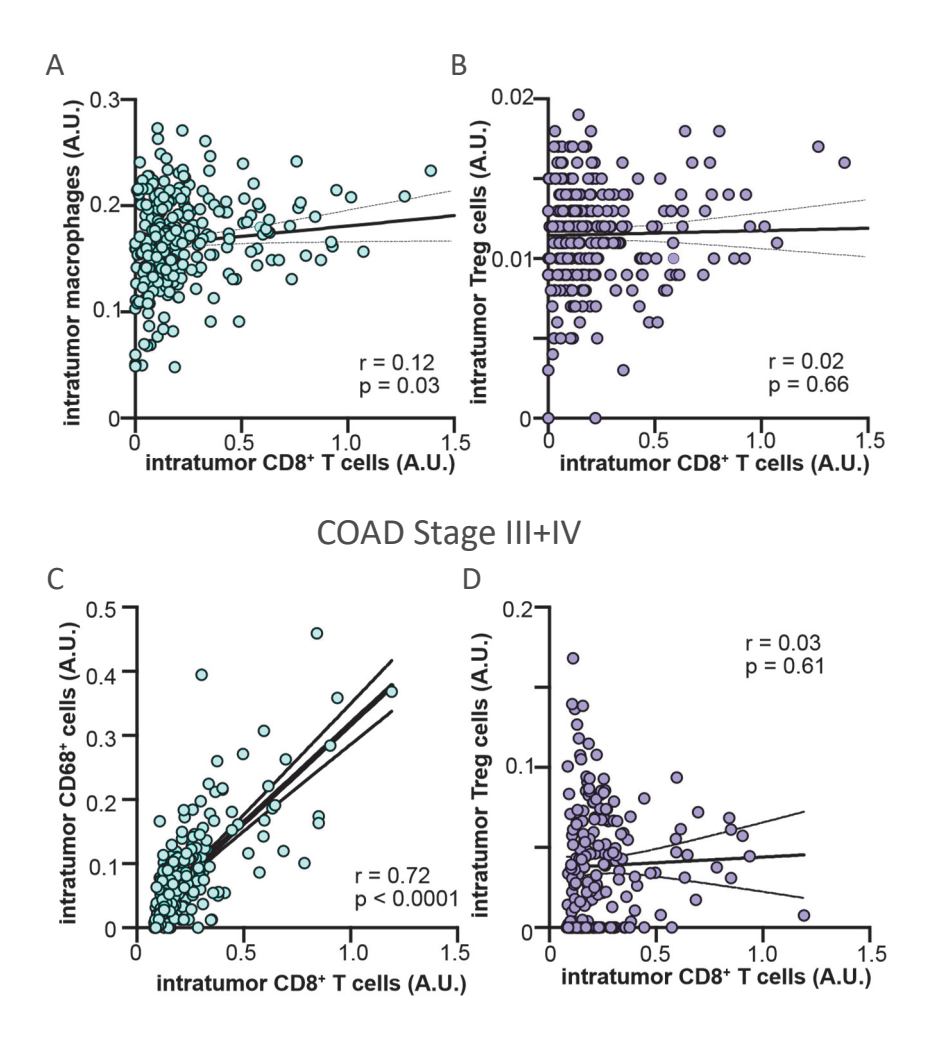
Suppl. Figure S2. Spatial localization of the immune cell subtypes in CRC tumors.Representative immunofluorescence images from three CRC tumor samples stained for CD8⁺ T cells (red), CD68⁺ macrophages (green), and FoxP3⁺ regulatory T cells (cyan). Merged images show triple labeling, and nuclei are counterstained with DAPI (blue). Scale bar: 50 μm.



Suppl. Figure S3. Intratumor CD8⁺ T cell density determines patient prognosis.

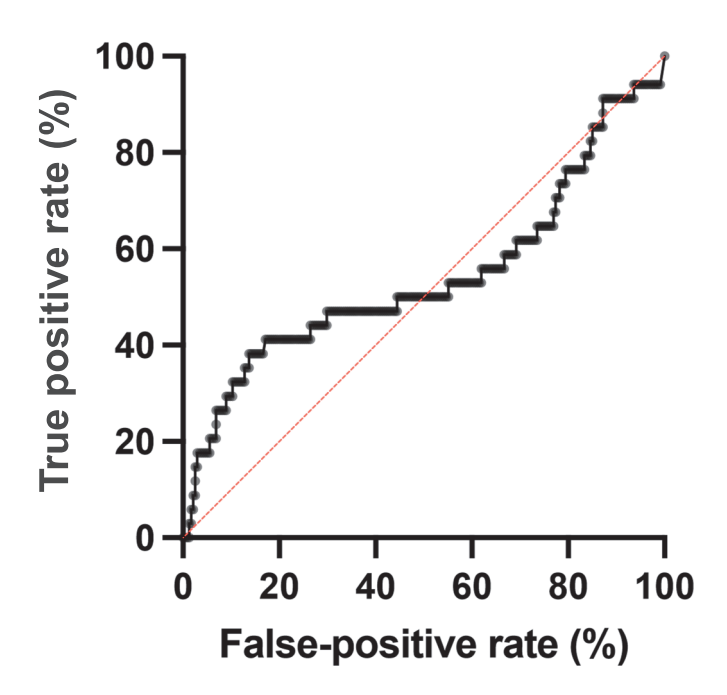
KaplanMeier curves and numbers of patients at risk in the study cohort, showing cumulative RFS probability for patients grouped by intratumor CD8⁺T cell density (cells/mm²). Unadjusted relapse estimates at 4 and 7 years for all groups are shown.

COAD Stage I+II



Suppl. Figure S4. Correlations between immune cell subtypes in the COAD cohort.

Regression analysis between intratumor CD8⁺ T cell density and tumor-infiltrating macrophages (A, C) or Treg cells (B, D) in tumors from the COAD cohort stage I/II (A, B) or III/IV (C, D). The correlation coefficient and the p-value are shown in each graph. Statistical tests: two-tailed Pearson's correlation coefficient.



Suppl. Figure S5. ROC curve for CD8⁺ T cell abundance and OS in the COAD stage I-II cohort. The ROC curve (black line) evaluates the ability of CD8⁺ T cell abundance in tumors to predict OS. The red diagonal line represents a random classifier (area under the curve = 0.5). The curve's proximity to this diagonal suggest a limited prognostic value of CD8⁺ T cell abundance for OS.

Suppl. Table S1. Demographic and clinical characteristics of the study cohort

| Characteristic | | Value | |
|------------------|---------------------------|-------------------|--|
| Age (median, SD) | | 73.03 (9.6) years | |
| Gender (%, nun | nber) | | |
| | Female | 40% (38) | |
| | Male | 60% (57) | |
| Location | | | |
| | Cecum | 13.7% (13) | |
| | Right colon | 26.3% (25) | |
| | Transverse colon | 7.4% (7) | |
| | Left colon | 5.3% (5) | |
| | Sigmoid colon | 25.3% (24) | |
| | Rectum | 22.1% (21) | |
| Mucinous | | | |
| | Yes | 9.5% (9) | |
| | No | 90.5% (86) | |
| Grade | | | |
| | Well differentiated | 18.9% (18) | |
| | Moderately differentiated | 72.6% (69) | |
| | Poorly differentiated | 8.4% (8) | |
| T Stage | | | |
| | T1 | 3.2% (3) | |
| | T2 | 31.6% (30) | |
| | Т3 | 64.2% (61) | |
| | T4 | 1.1% (1) | |
| Recurrence | | | |
| | Yes | 31.6% (30) | |
| | No | 68.4% (65) | |
| Time to recur | rence (median) | 19 months | |

Suppl. Table S2. Demographic and clinical characteristics of the validation cohort

| Characteristic | | Value |
|------------------|---------------------------|-------------------|
| Age (median, SD) | | 75.0 (12.5) years |
| Gender (%, nun | nber) | |
| | Female | 40.3% (91) |
| | Male | 59.7% (135) |
| Location | | |
| | Cecum/Right colon | 41.1% (93) |
| | Transverse colon | 5.3% (12) |
| | Left/Sigmoid colon | 36.3% (82) |
| | Rectum | 17.2% (39) |
| Mucinous | | |
| | Yes | 9.7% (22) |
| | No | 90.3% (204) |
| Grade | | |
| | Well differentiated | 15.0% (34) |
| | Moderately differentiated | 75.7% (171) |
| | Poorly differentiated | 9.3% (21) |
| T Stage | | |
| | T1 | 0% (0) |
| | T2 | 14.7% (33) |
| | Т3 | 81.8% (185) |
| | T4 | 3.5% (8) |
| Recurrence | | |
| | Yes | 18.6% (42) |
| | No | 81.3% (183) |
| Time to recurr | rence (median) | 17.2 months |

Suppl. Table S3. Demographic and clinical characteristics of the COAD stage I+II cohort

| Characteristic | | Value |
|------------------|---------------------------|-------------------|
| Age (median, SD) | | 70.5 (12.4) years |
| Gender (%, nu | ımber) | |
| | Female | 53.3% (144) |
| | Male | 46.7% (126) |
| Location | | |
| | Cecum | 19.6% (53) |
| | Right colon | 27.4% (74) |
| | Transverse colon | 4.4% (12) |
| | Left colon | 3.3% (9) |
| | Sigmoid colon | 21.5% (58) |
| | Rectum | 23.7% (64) |
| Mucinous | | |
| | Yes | 13.3% (36) |
| | No | 86.7% (234) |
| Grade | | |
| | Well differentiated | 29.6% (80) |
| | Moderately differentiated | 70.4% (190) |
| | Poorly differentiated | 0% (0) |
| T Stage | | |
| | Tis | 0.4% (1) |
| | T 1 | 3.7% (10) |
| | T2 | 26.3% (71) |
| | Т3 | 64.4% (174) |
| | T4 | 5.2% (14) |
| Survival | | |
| | Yes | 87.4% (236) |
| | No | 12.6% (34) |

| Time to death (median) | 24.33 months |
|------------------------|--------------|
| | |

Suppl. Table S4. Demographic and clinical characteristics of the COAD stage III+IV cohort

| Characteristic | | Value | |
|------------------|-----------------------|-----------------|--|
| Age (median, SD) | | 66 (13.5) years | |
| Gender (%, nu | amber) | | |
| | Female | 51.2% (106) | |
| | Male | 48.8% (101) | |
| Location | | | |
| | Cecum | 20.3% (42) | |
| | Right colon | 16.4% (34) | |
| | Transverse colon | 5.3% (11) | |
| | Left colon | 4.3% (9) | |
| | Sigmoid colon | 32.4% (67) | |
| | Rectum | 21.3% (44) | |
| Mucinous | | | |
| | Yes | 15.9% (33) | |
| | No | 83.5% (173) | |
| Grade | | | |
| | Poorly differentiated | 65.2% (135) | |
| | Undifferentiated | 32.4% (67) | |
| | Not specified | 2.4% (5) | |
| T Stage | | | |
| | T1 | 0.5% (1) | |
| | T2 | 4.8% (10) | |
| | T3 | 72.9% (151) | |
| | T4 | 21.7% (45) | |

| Survival | |
|------------------------|--------------|
| Yes | 66.7% (138) |
| No | 33.4% (69) |
| Time to death (median) | 22.07 months |

Suppl. Table S5. Multivariate Cox regression analysis of disease-free survival in our study cohort

| Variables | HR | 95% CI | z-stats | p-val |
|--------------------------------|------|-----------|---------|-------|
| Age | 0.99 | 0.95 1.03 | -0.39 | 0.70 |
| Sex | 0.99 | 0.42 2.32 | -0.02 | 0.99 |
| Mucinous (y/n) ^a | 0.00 | 0.00 inf | -0.01 | 1.00 |
| Tumor site | 1.99 | 0.78 1.28 | -0.01 | 0.99 |
| Grade | 1.11 | 0.49 2.52 | 0.26 | 0.79 |
| T-stage | 0.87 | 0.38 2.00 | -0.33 | 0.74 |
| Lam-α4 z-score | 1.00 | 1.00 1.01 | 1.02 | 0.31 |
| CD8 ⁺ T cell number | 0.96 | 0.93 0.99 | -2.54 | 0.01 |
| FoxP3+T cell number | 1.00 | 0.95 1.05 | -0.12 | 0.91 |
| CD68+ cell number | 0.95 | 0.90 1.02 | -1.43 | 0.15 |

Concordance: 0.73. -log2(p) of likelihood ratio test: 7.18 ^aThe variable mucinous histology yielded an unusual result, likely due to a lack of events or insufficient representation in this subgroup.

Suppl. Table S6. Multivariate Cox regression analysis of disease-free survival in CD8-high tumors from the study cohort

| Variables | HR | 95 | % CI | z-stats | p-val |
|-------------------------------|------|------|-------|---------|-------|
| CD8 high density tumo | rs | | | | |
| Age | 1.10 | 0.92 | 1.31 | 1.02 | 0.38 |
| Sex | 1.80 | 0.30 | 10.97 | 0.64 | 0.52 |
| Mucinous (y/n) a | 0.00 | 0.00 | inf | -0.01 | 0.99 |
| Tumor site | 0.43 | 0.20 | 0.92 | -2.18 | 0.03 |
| Grade | 1.05 | 0.16 | 6.76 | 0.06 | 0.96 |
| T-stage | 0.92 | 0.12 | 7.26 | -0.08 | 0.94 |
| Lam-α4 z-score | 1.00 | 0.99 | 1.02 | 0.16 | 0.87 |
| FoxP3+T cell number | 1.22 | 1.05 | 1.41 | 2.56 | 0.01 |
| CD68 ⁺ cell number | 0.79 | 0.63 | 0.98 | -2.18 | 0.03 |

Concordance: 0.90. -log2(p) of likelihood **ratio** test: 6.11 ^aThe variable mucinous histology yielded an unusual result, likely due to a lack of events or insufficient representation in this subgroup.

Suppl. Table S7. Univariate Cox regression analysis of disease-free survival for the indicated variables in CD8-high tumors

| Variables | HR | 95% CI | | z-stats | p-val |
|----------------------------------|------|--------|------|---------|-------|
| CD8 high density tumo | ors | | | | |
| Tumor site | 0.74 | 0.46 | 1.20 | -1.21 | 0.23 |
| FoxP3 ⁺ T cell number | 1.05 | 0.98 | 1.11 | 1.40 | 0.16 |
| CD68 ⁺ cell number | 0.91 | 0.81 | 1.02 | -1.70 | 0.09 |

Concordance: 0.83. -log2(p) of likelihood ratio test: 4.10

Supp. Table S8. Multivariate Cox regression analysis of disease-free survival in CD8-low tumors from the study cohort

| Variables | HR | 95% CI | | z-stats | p-val |
|-------------------------------|------|--------|------|---------|-------|
| CD8 low density tumo | | | | | |
| Age | 0.98 | 0.94 | 1.03 | -0.88 | 0.38 |
| Sex | 0.54 | 0.18 | 1.65 | -1.08 | 0.28 |
| Mucinous (y/n) ^a | 0.00 | 0.00 | inf | -0.00 | 1.00 |
| Tumor site | 1.11 | 0.81 | 1.50 | 0.64 | 0.52 |
| Grade | 0.51 | 0.13 | 2.02 | -0.96 | 0.34 |
| T-stage | 1.91 | 0.55 | 6.61 | 1.02 | 0.31 |
| Lam-α4 z-score | 1.00 | 1.00 | 1.01 | 0.89 | 0.37 |
| FoxP3+T cell number | 0.95 | 0.89 | 1.02 | -1.34 | 0.18 |
| CD68 ⁺ cell number | 1.00 | 0.91 | 1.10 | 0.03 | 0.97 |

Concordance: 0.67. -log2(p) of likelihood **ratio** test: 1.86 ^aThe variable mucinous histology yielded an unusual result, likely due to a lack of events or insufficient representation in this subgroup.

Supp. Table S9. Multivariate Cox regression analysis of disease-free survival in the validation cohort

| Variables | HR | 95% CI | | c CI z-stats | |
|-------------------------------|------|--------|------|--------------|---------|
| Age | 1.01 | 0.98 | 1.04 | 0.44 | 0.66 |
| Sex | 0.34 | 0.13 | 0.67 | -2.25 | 0.02 |
| Mucinous (y/n) | 1.69 | 0.54 | 5.34 | 0.90 | 0.37 |
| Tumor site | 0.91 | 0.64 | 1.28 | -0.55 | 0.58 |
| Grade | 0.80 | 0.34 | 1.90 | -0.50 | 0.61 |
| T-stage | 2.79 | 1.06 | 7.18 | 2.13 | 0.03 |
| Lam-α4 z-score | 1.00 | 0.99 | 1.01 | 0.10 | 0.92 |
| CD8+T cell number | 0.96 | 0.94 | 0.99 | -2.97 | < 0.005 |
| FoxP3+T cell number | 1.07 | 1.01 | 1.13 | 2.22 | 0.03 |
| CD68 ⁺ cell number | 0.96 | 0.95 | 1.02 | -1.70 | 0.09 |

Suppl. Table S10. Multivariate Cox regression analysis of disease-free survival in CD8-high tumors from the validation cohort

| Variables | HR | 959 | % CI | z-stats | p-val |
|-------------------------------|------|------|------|---------|-------|
| CD8 high density tumo | rs | | | | |
| Age | 1.01 | 0.96 | 1.06 | 0.23 | 0.81 |
| Sex | 0.79 | 0.17 | 3.64 | -0.30 | 0.77 |
| Mucinous (y/n) a | 0.00 | 0.00 | inf | -0.01 | 1.00 |
| Tumor site | 0.90 | 0.52 | 1.56 | -0.37 | 0.71 |
| Grade | 0.62 | 0.18 | 2.16 | -0.74 | 0.46 |
| T-stage | 4.45 | 0.95 | 20.7 | 1.90 | 0.06 |
| Lam-α4 z-score | 1.00 | 0.99 | 1.01 | 0.26 | 0.79 |
| FoxP3+T cell number | 1.07 | 1.05 | 1.14 | 2.04 | 0.04 |
| CD68 ⁺ cell number | 0.94 | 0.88 | 0.98 | -2.04 | 0.04 |

^aThe variable mucinous histology yielded an unusual result, likely due to a lack of events or insufficient representation in this subgroup.

Supp. Table S11. Multivariate Cox regression analysis of disease-free survival in CD8-low tumors from the validation cohort

| Variables | HR | 95% CI | | z-stats | p-val | | | | |
|----------------------------------|------|--------|------|---------|-------|--|--|--|--|
| CD8 low density tumors | | | | | | | | | |
| Age | 1.01 | 0.97 | 1.06 | 0.62 | 0.53 | | | | |
| Sex | 0.32 | 0.10 | 1.00 | -1.96 | 0.05 | | | | |
| Mucinous (y/n) | 0.93 | 0.56 | 1.54 | -0.28 | 0.78 | | | | |
| Tumor site | 1.38 | 0.86 | 2.21 | 1.32 | 0.19 | | | | |
| Grade | 1.11 | 0.29 | 4.21 | 0.15 | 0.88 | | | | |
| T-stage | 3.12 | 0.98 | 9.92 | 1.93 | 0.05 | | | | |
| Lam-α4 z-score | 1.00 | 0.99 | 1.01 | -0.55 | 0.58 | | | | |
| FoxP3 ⁺ T cell number | 1.03 | 0.93 | 1.13 | 0.50 | 0.62 | | | | |
| CD68 ⁺ cell number | 1.00 | 0.98 | 1.03 | 0.29 | 0.77 | | | | |

Suppl. Table S12. Multivariate Cox regression analysis of overall survival in the COAD cohort stage I + II (all data)

| Variables | HR | <u>95</u> % CI | z-stats | p-val |
|--------------------------------------|------|--------------------|---------|-------|
| Age | 1.06 | 1.01 1.11 | 2.57 | 0.01 |
| Sex | 1.64 | 0.77 3.50 | 1.27 | 0.20 |
| Mucinous (y/n) | 1.40 | 0.54 3.63 | 0.69 | 0.49 |
| Tumor site | 1.03 | 0.91 1.15 | 0.42 | 0.68 |
| Grade | 2.10 | 0.28 15.89 | 0.72 | 0.47 |
| T-stage | 0.85 | 0.18 3.98 | -0.21 | 0.83 |
| LAMA4 mRNA | 1.00 | 0.97 1.03 | -0.20 | 0.84 |
| CD8 ⁺ T cell infiltration | 2.68 | 1.19 6.04 | 2.38 | 0.02 |
| Treg cell infiltration | 0.00 | $0.00 	 10^{36}$ | -0.76 | 0.45 |
| macrophage infiltration | 0.00 | <u>0.00</u> 376.76 | -0.95 | 0.34 |

Concordance: 0.74

Suppl. Table S13. Multivariate Cox regression analysis of overall survival in the COAD cohort stage I + II (excluded high CD8 infiltration)

| Variables | HR | <u>95</u> 9 | 6 CI | z-stats | p-val |
|--------------------------------------|------|-------------|--------------------|---------|-------|
| Age | 1.07 | 1.02 | 1.13 | 2.80 | 0.01 |
| Sex | 2.94 | 1.15 | 7.50 | 2.25 | 0.02 |
| Mucinous (y/n) | 2.25 | 0.90 | 5.57 | 1.74 | 0.08 |
| Tumor site | 0.93 | 0.80 | 1.07 | -1.03 | 0.30 |
| Grade | 1.34 | 0.13 | 14.22 | 0.24 | 0.81 |
| T-stage | 1.00 | 0.16 | 6.28 | -0.00 | 1.00 |
| LAMA4 mRNA | 1.02 | 0.98 | 1.06 | 0.81 | 0.42 |
| CD8 ⁺ T cell infiltration | 3.36 | 0.16 | 70.16 | 0.78 | 0.44 |
| Treg cell infiltration | 0.00 | 0.00 | 8x10 ₃₄ | -0.99 | 0.32 |
| macrophage infiltration | 0.00 | 0.00 | 675.52 | -0.99 | 0.32 |

Concordance: 0.78